



Origin and geochemical evolution of groundwater in the Abaya Chamo basin of the Main Ethiopian Rift: application of multi-tracer approaches

Muhammed Haji^{1,2,3} · Dajun Qin^{2,3} · Yi Guo^{2,3} · Lu Li^{2,3} · Dongdong Wang^{2,3} · Shankar Karuppanan¹ · Hassen Shube¹

Received: 18 February 2020 / Accepted: 9 December 2020 / Published online: 28 January 2021
© Springer-Verlag GmbH Germany, part of Springer Nature 2021

Abstract

The fractured volcanic aquifer of the Abaya Chamo basin in the southern Ethiopian Rift represents an important source for water supply. This study investigates the geochemical evolution of groundwater and the groundwater flow system in this volcanic aquifer system using hydrochemistry and environmental tracers. Water types of groundwater were found to transform from Ca-Mg-HCO₃ (western part of Lake Abaya area) to Na-HCO₃ (northwestern part), from the highland down to the Rift Valley. Silicate hydrolysis and Ca/Na ion exchange are the major geochemical processes that control groundwater chemistry along the flow path. Groundwaters are of meteoric origin. The $\delta^{18}\text{O}$ and δD content of groundwater ranges from -4.9 to -1.1‰ and -27 to 5‰ , respectively. The $\delta^{18}\text{O}$ and δD values that lie on the summer local meteoric water line indicate that the groundwater was recharged mainly by summer rainfall. $\delta^{13}\text{C}_{\text{DIC}}$ values of cold groundwater range from -12 to -2.7‰ , whereas $\delta^{13}\text{C}_{\text{DIC}}$ of thermal groundwater ranges from -8.3 to $+1.6\text{‰}$. The calculated $\delta^{13}\text{C}_{\text{CO}_2(\text{g})}$ using $\delta^{13}\text{C}_{\text{DIC}}$ and DIC species indicates the uptake of soil CO₂ for cold groundwater and the influx of magmatic CO₂ through deep-seated faults for thermal groundwater. In the western part of Lake Abaya area, the shallow and deep groundwater are hydraulically connected, and the uniform water type is consistent with a fast flow of large gradient. In contrast, in the northern part of Lake Abaya area, water underwent deep circulation and slow flow, so the water types—e.g. high F⁻ (up to 5.6 mg/L) and Na⁺—varied laterally and vertically.

Keywords Volcanic aquifer · Hydrochemistry · Stable isotopes · Water · Rock interaction · Groundwater flow · Ethiopia

Introduction

Volcanic aquifers constitute major water resources in many parts of the world, including France (Bertrand et al. 2010), Portugal (Cruz and Silva 2001; Prada et al. 2016), Israel (Dafny et al. 2003), Mexico (Carrillo-Rivera et al. 2007; Ochoa-González et al. 2015), Brazil (Gastmans et al. 2016), India (Kulkarni

et al. 2000), South Korea (Koh et al. 2009), Cameroon (Ako et al. 2013) and Kenya (Olaka et al. 2016). Particularly in Ethiopia, groundwater originating from volcanic terrain serves as a vital source for water supply (Demlie et al. 2008; Kebede et al. 2010); however, the potential of groundwater varies significantly owing to the complex geological condition of the volcanic rocks. Many volcanic rocks possess extremely heterogeneous structure and are chemically more reactive, due to the existence of fine particles and the abundance of vitreous matter (Asai et al. 2009), which results in complex flow and lithogenic contaminants in groundwater including F and As (Cordeiro et al. 2012; Vivona et al. 2007). Despite its potential for variation, groundwater in the volcanic aquifers will continue to be exploited.

Studies on volcanic aquifers have been carried out in relation to the aspects of groundwater recharge (Demlie et al. 2007), origin and flow dynamics (Bertrand et al. 2010; Bretzler et al. 2011; Demlie et al. 2008; Kebede et al. 2008; Mechal et al. 2016; Rango et al. 2010), water quality (Ayenew

✉ Muhammed Haji
mohehaji@gmail.com

¹ School of Applied Natural Science, Adama Science and Technology University, P.O. Box 1888, Adama, Ethiopia

² Key Laboratory of Shale Gas and Geoenvironment, Institute of Geology and Geophysics, Chinese Academy of Sciences, Beijing 100029, China

³ Institute of Earth Science, Chinese Academy of Sciences, Beijing, China

2008; Cordeiro et al. 2012; Furi et al. 2011; Gizaw 1996; Rango et al. 2008; Reimann et al. 2003), water–rock interaction, (Darling et al. 1996; Dietzel and Kirchhoff 2002; Koh et al. 2017), geochemical evolution (Alemayehu et al. 2011; Cruz and França 2006; Gastmans et al. 2016; Vaselli et al. 2002), groundwater age (Ako et al. 2013) and source of dissolved carbon (Bertrand et al. 2013; Cartwright et al. 2002). Nevertheless, characterization of the groundwater flow system and geochemical evolution of volcanic aquifers is hydrogeologically challenging. This is mainly due to the heterogeneity and anisotropy of volcanic aquifers that resulted from the accumulation of lava and pyroclastic flows, the fracturing of volcanic rocks, different degrees of weathering, and the disruption of lithologies by tectonic activity (Kebede et al. 2008; Möller et al. 2016).

The Ethiopian Rift System is a classic example of a continental rift where recent and active deformation, as well as volcanic activity, has occurred. As a consequence of the tectonic activity, the typical rift morphology is well developed and widespread basaltic and rhyolitic volcanic activity has occurred since the Miocene (Corti 2009; WoldeGabriel et al. 1990). This in turn has resulted in highly variable topography and climate within short distances, and highly variable stratigraphic sequences (both vertically and laterally) that are dissected by faults. The interplay of tectonic and volcanic activities in the Ethiopian Rift System resulted in complex hydrogeological settings (Haile and Abiye 2012), where there exists: large heterogeneity of aquifers (e.g. variable water levels) in short distances (Ayenew et al. 2008; Furi et al. 2010; Kebede et al. 2010; Rango et al. 2010); spatial variation of fluoride in groundwater (Chernet et al. 2001; Rango et al. 2008; Reimann et al. 2003; Tekle-Haimanot et al. 2006); geothermal anomalies (Haile and Abiye 2012) and a laterally discontinuous aquifer (Kebede et al. 2008). Similarly, aquifer productivity and water-table depth differ significantly over short distances (Ayenew et al. 2008; Furi et al. 2010). A sound understanding of the hydrogeological setting is therefore required for an adequate development of groundwater resources in the Ethiopian Rift.

In the past few decades, hydrogeological studies mainly focused on the central Main Ethiopian Rift. Groundwater flow dynamics and hydro-geochemistry (Bretzler et al. 2011; Demlie et al. 2008; Kebede et al. 2005; Rango et al. 2010), and fluoride distribution (Ayenew 2008; Tekle-Haimanot et al. 2006) and its relationship with dental and skeletal fluorosis (Rango et al. 2012; Tekle-Haimanot and Haile 2014; Wondwossen et al. 2004), were investigated in the central Main Ethiopian Rift. In contrast, the existing hydrogeological investigations in Abaya Chamo basin of the southern Main Ethiopian Rift, have involved reconnaissance surveys limited to groundwater resource investigations (Halcrow 2008; JICA 2012; UNDP 1973) and study of the limnology of Abaya and Chamo Lake (e.g. Zinabu et al. 2002). Only recently, Haji et al.

(2018) employed hydrochemistry to assess the fluoride enrichment mechanism; yet very little is known about the detailed hydrogeology of the area. In the present study, groundwater in a volcanic aquifer of the southern part of the Main Ethiopian Rift (MER), the Abaya Chamo Lake Basin, was investigated focusing on the groundwater origin and geochemical evolution. The selected area represents the southwestern flank of the MER where geological formations, tectonic structures and relief features are highly complex and characterized by wide climate variation ranging from humid in the highland to semiarid on the rift floor (Haji et al. 2018).

Hydrochemical and isotopic information on groundwater has been widely used to understand complex groundwater flow systems (Bretzler et al. 2011; Mechal et al. 2016; Qin et al. 2017) in response to tectonic structure, lithologic variation and climate condition. Stable isotopes ($\delta^{18}\text{O}$ and δD) can be used as tracers of groundwater origin, mixing of waters of different origins, and recharge conditions and flow pathways (Clark 2015; Négrel et al. 2016), and ideal tracers for determining groundwater flow paths, as they are an intrinsic component of the water molecule (Qin et al. 2017). $\delta^{13}\text{C}$ is commonly used in groundwater studies and its analysis serves as a powerful tool for identifying carbon sources and fluxes because the carbon reservoirs have distinctively different isotope ratios (Genereux et al. 2009; Koh et al. 2017). On the other hand, major ion chemistry helps to define chemical reactions, acquired by water–rock interaction, that control groundwater composition (Ahmed and Clark 2016; Belkhiri et al. 2012; Gastmans et al. 2016). Combining hydrochemistry and environmental tracer data allows for constraining groundwater flow paths and geochemical evolution and is also helpful to identify different groundwater flow systems.

The purpose of this study is to investigate groundwater geochemical evolution and the origin of groundwater in volcanic areas and to establish a conceptual hydrogeological model in the study area. To facilitate this, multiple isotopes ($\delta^{13}\text{C}$, $\delta^{18}\text{O}$ and δD) in conjunction with hydrochemical data were used. These efforts were integrated with the interpretation of information on the lithologic and hydrologic setting of the area, to establish a hydrogeological conceptual model considering both groundwater flow paths and chemical evolution.

This report reports the first determination of the origin and geochemical evolution of groundwater in the southern part of the Main Ethiopian Rift, Abaya Chamo basin, using multiple environmental tracers ($\delta^{13}\text{C}$, $\delta^{18}\text{O}$ and δD) and hydrochemical information. On the basis of these data, this report documents the (1) geochemical processes associated with the groundwater (2) groundwater origin (3) source of dissolved inorganic carbon and (4) groundwater flow system in the fractured volcanic aquifers of western Abaya Chamo basin. It is anticipated that this study will provide valuable information about the hydrogeology of this complex volcanic aquifer system which could be useful for the sustainable

management of its groundwater resources. For future hydrogeological research, the present study would be helpful in improving the understanding of groundwater origin, geochemical evolution, flow processes and quality distribution.

Geological and hydrogeological aspects of the study area

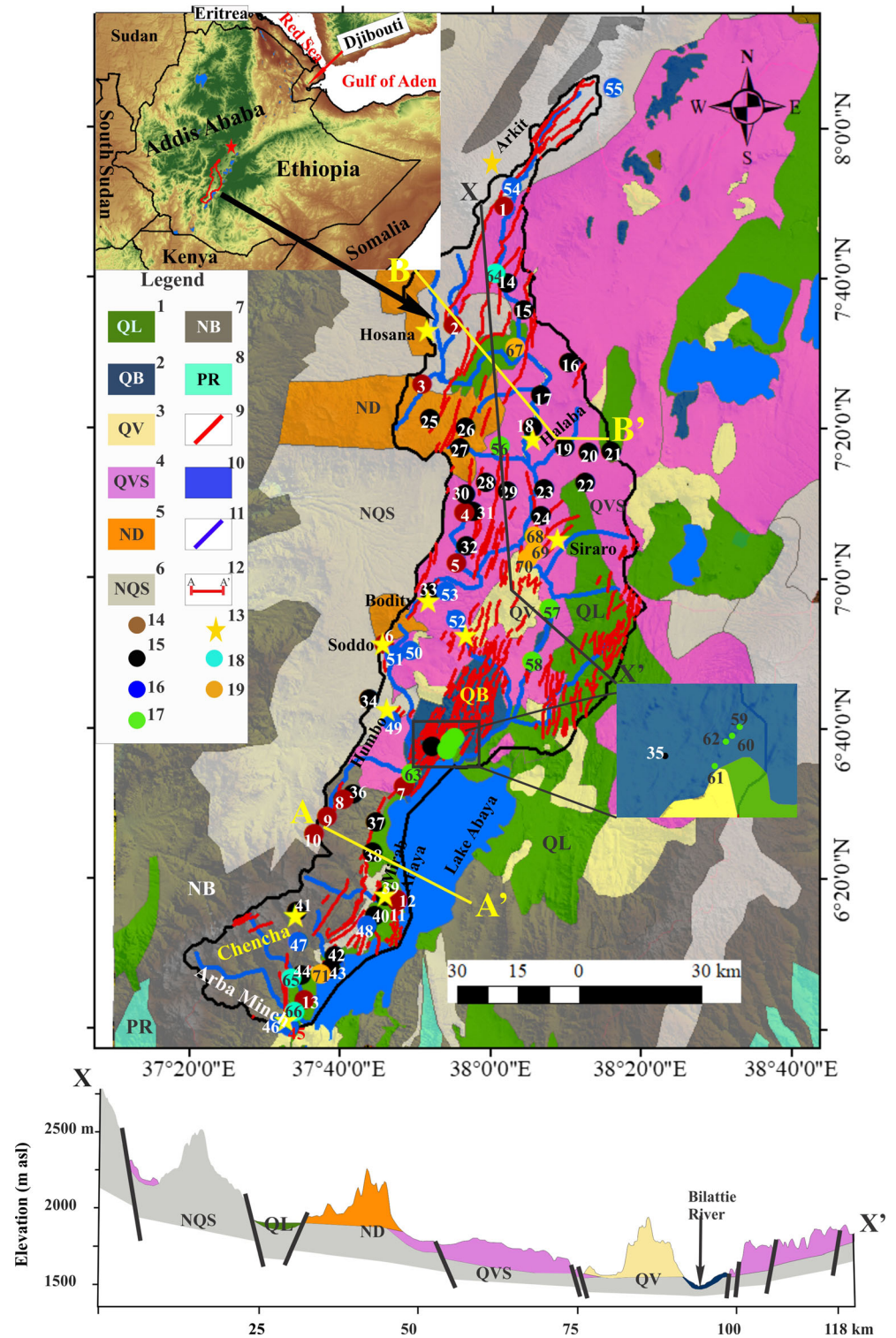
The study area ($5^{\circ}25'0''$ – $8^{\circ}5'0''$ N latitude and $37^{\circ}16'00''$ – $38^{\circ}40'0''$ E longitude) is located on the western margin of the southern MER, extending from the southern coast of Lake Abaya to the town of Arkit, as shown in Fig. 1. The study area has a semiarid climate on the rift floor and humid climate in the eastern and western highlands. The annual rainfall in the rift varies widely from around 800 within the rift to 1,500 mm in large parts of the highlands. In the lowland of Arba Minch, in the vicinity of Lake Abaya, the mean annual rainfall is 880 mm. The mean annual rainfall in the western highland is as high as 1,541 mm. A bimodal rainfall pattern (March–May and July–October) is found in the study area. The average monthly temperatures on the rift floor and the high-elevation plateau (highland) are 22 and 14 °C, respectively.

In addition to sediments and lacustrine deposits, the basin is covered by Tertiary and Quaternary volcanism. The oldest volcanic rocks (Oligocene to middle Miocene) are found in the study area. The volcanic rocks are distributed considerably in the highland and slightly in the rift floor (Corti et al. 2013). These volcanic rocks comprise of basaltic lava flows and inter-stratified ignimbritic beds, covered by massive rhyolites and interfering tuffs and basalts (NB in Fig. 1). The basaltic rocks are intensely jointed and weathered and are mainly exposed around Chench highlands. The radiometric ages range from 45 to 27 Ma in the basalts and from 37 to 27 Ma in the rhyolites (Ebinger et al. 1993; WoldeGabriel et al. 1991; Zanettin et al. 1978). Rift volcanic rocks (Pliocene) are commonly found in the rift floor and highlands, which consists of peralkaline pantelleritic ignimbrites with subordinate unwelded tuffs, ash flows, rhyolites, and trachytes, as shown with label NQS in Fig. 1. The units of pyroclastic rocks in the area are found to be similar to those in the northern and central MER (Corti et al. 2013). The radiometric age of 4.2–2.5 Ma is obtained for these units in the study area (WoldeGabriel et al. 1990). The large flows of trachytic lava from Damota volcanic centre overlie the Nazareth pyroclastic rocks (ND in Fig. 1). The trachytic lava is of late Pliocene and 2.9 Ma age (WoldeGabriel et al. 1990). In Pleistocene, volcanic sediments over the rift floor are formed with alluvial and pumiceous tuff that contains rhyolite and welded tuff fragments, lacustrine strata, and minor basalt flows (Corti et al. 2013; WoldeGabriel et al. 1990; Zanettin et al. 1978; QVS in Fig.

1). Pyroclastic materials are mainly Quaternary eruptive from vents such as Hobitcha (Chernet 2011) and Corbetti (Rapprich et al. 2016). The youngest volcanic units (Pleistocene–Holocene) are associated with obsidian flows, ignimbrite, pumice, rhyolitic flows and domes, pyroclastic surge deposits, scattered basaltic lava flows and spatters cones (QV in Fig. 1). Basaltic lava and scoria cones are distributed along NNE trending faults (Chernet 2011; Corti et al. 2013). Radiometric dating of 1.57 Ma was reported for the rhyolite taken from the inner caldera rim of Hobticha (Chernet 2011). More recent Quaternary volcanic units crop out in the area, which mostly occupies the land between Lake Abaya and Duguna (QB in Fig. 1). The Quaternary volcanic units are made up of basaltic lava flows, scoria, and phreatomagmatic deposits that are associated with the recent fault systems affecting the Rift Valley, usually referred to as the Wonji Fault Belt, WFB (Ebinger et al. 1993; Rooney et al. 2011; Zanettin et al. 1978). The most recent deposits in the area are Holocene sediments, which consist of lacustrine and fluvial sediment deposited by Lake Abaya and two major rivers (Bilattie and Gidabo), respectively (QL in Fig. 1). A lacustrine delta of a few kilometers is widely spread in the northern part of Lake Abaya area. The thickness of sediments varies from 8 to 20 m around the confluence of Bilate River and Lake Abaya.

The aquifers of the basin are characterized by fractured volcanic rocks, sediments and lacustrine deposits of Tertiary and Quaternary age. Quaternary deposits in the rift floor form shallow aquifers, with water yield that varies between 3 and 14 L/s (Alemayehu 2006; Kebede 2013). The yield in the Quaternary fissured volcanic aquifers varies from 2 to 5 L/s (Alemayehu 2006; Ayenew et al. 2008; Kebede et al. 2016). Weathered volcanic rocks together with locally inter-bedded gravels and alluvial deposits form the water-yielding zones in the upland area. The alluvium-lacustrine sediments, particularly in the upper Bilate River, have medium to high permeability and productivity, where the groundwater wells can yield up to 9 L/s with varying water tables from 1.5 to 50 m (Kebede 2013). Water-bearing units in the Lake Abaya area are primarily composed of fractured and weathered basalts, ignimbrites, and lacustrine and alluvial sediments. The depth of the water table varies with an increasing trend from the highland towards the rift floor. The depth of the static water level in the highland and escarpment ranges from just below the land surface to approximately 40 m, while on the rift floor it can reach up to 290 m below ground level (bgl). The volcanic terrain of Ethiopia is characterized by the occurrence of numerous springs that yield between 2 L/s (in dry areas) and 250 L/s (Alemayehu 2006). Springs at the foot of the escarpment are largely representing shallow and deep groundwater flows, e.g. Arbaminch Spring yields 250 L/s (Alemayehu 2006). The use of groundwater in the southern Main Ethiopian Rift is hindered by its poor water quality, which is associated with elevated fluoride concentrations that exceeds

Fig. 1 Simplified geological map of the Abaya Chamo basin (compiled and modified from Corti et al. 2013; Molin and Corti 2015) and cross-section X–X'. General legend: 1 (QL): lacustrine deposit; 2 (QB): recent basalt; 3 (QV): rhyolitic volcanic complex; 4 (QVS): rift floor pyroclastic deposits; 5 (ND): damota trachyte; 6 (NQS): Nazareth pyroclastic rock; 7 (NB): pre-rift basalt; 8 (PR): Precambrian basement; 9: faults; 10: lake; 11: river; 12: cross section; 13: town. Legend for sample symbols (colored circles with sample number): 14: shallow well; 15: deep well; 16: cold spring; 17: hot spring; 18: river water and 19: lake water



1.5 mg/L (Haji et al. 2018). In relation to active fault zones, many thermal springs emerge in the area, particularly in the tectonically active rift floor of the northern Abaya Lake. The thermal springs discharge within the rift floor along the NNE–SSW-trending faults (Minissale et al. 2017)

that emerge at varying elevation. Thermal springs in the northern Abaya Lake area are characterized by a temperature ranging from 35 to 95 °C and Na-HCO₃ type (Craig et al. 1977; Minissale et al. 2017) with a TDS in the range of 1,000–2,500 mg/L.

Methodology

Sampling and analytical techniques

This study is based on water sample analysis together with the utilization of existing geological and hydrogeological information. An effective water sampling campaign was undertaken through the area for hydrochemical and isotope analysis. The selection of the sampling locations took into consideration the presence of a complex water flow system, where cold water and thermal springs are found together. As shown in Figs. 1, 71 water samples were collected from supply wells, springs, rivers and lakes for the study. In brief, 13 samples were collected from shallow wells (10–60 m), 31 samples from deep wells (60–360 m), 11 samples from cold springs, 8 samples from hot springs, 3 samples from rivers and 5 samples from lakes. Samples were taken from supply taps, or as close as possible to the well head while the pump runs to ensure the sampling of primary groundwater. Duplicate samples were collected for the analysis of major ions and isotopes. Samples were stored in new 100-ml polyethylene bottles for major ions and 100-ml glass bottle for $\delta^{13}\text{C}_{\text{DIC}}$, $\delta^{18}\text{O}$ and δD analysis. Water temperature (T), pH and electrical conductivity (EC) were measured in situ using a portable multi-functional water quality analyzer (Multi 3430) that was calibrated before use.

Major ions (Ca^{2+} , Mg^{2+} , Na^+ , K^+ , SO_4^{2-} , Cl^- , F^- and NO_3^-) concentrations were measured using ion chromatography (Dionex Dx-120). Alkalinity was measured on the

sampling day by Gran titration using 0.05 M HCl. The accuracy of water analyses was checked by utilizing charge balance error ($\text{Charge balance error}\% = \frac{\sum_{\text{cation}} - \sum_{\text{anion}}}{\sum_{\text{cation}} + \sum_{\text{anion}}} \times 100$) (Appelo and Postma 2005; Clark 2015). Based on the reproducibility of replicate samples, the analytical precision is found to be within 5% in all water samples except for lake water that showed a difference of 11%. δD and $\delta^{18}\text{O}$ were measured on a laser absorption water isotope spectrometer analyzer (Picarro L2120-i). All δD and $\delta^{18}\text{O}$ values are expressed relative to the Vienna Standard Mean Ocean Water in ‰ and the measurement precisions were ± 0.5 and $\pm 0.2\text{‰}$ for δD and $\delta^{18}\text{O}$, respectively. The carbon isotopic compositions of the samples were determined using a stable isotope ratio mass spectrometer. Carbon isotopic compositions are expressed as the δ notation relative to Vienna Pee Dee Belemnite (VPDB) and the analytical reproducibility is $\pm 0.2\text{‰}$ for $\delta^{13}\text{C}_{\text{DIC}}$. The samples were analyzed in the Laboratory of Groundwater Dating, Institute of Geology and Geophysics, Chinese Academy of Sciences.

Gaseous $\delta^{13}\text{C}_{\text{CO}_2}$ calculation

The variation of $\delta^{13}\text{C}_{\text{DIC}}$ is due to temperature- and pH-dependent fractionation factors between $\delta^{13}\text{C}_{\text{CO}_2}$ and $\delta^{13}\text{C}_{\text{DIC}}$ species (H_2CO_3 , HCO_3^- , and CO_3^{2-}). It is possible to relate the $\delta^{13}\text{C}$ of the CO_2 source to $\delta^{13}\text{C}_{\text{DIC}}$ in groundwater. Having the fractionation factors in mind, it is possible to calculate the initial signature of the CO_2 source which dissolved in water using the fractionation equation of (Deines et al. 1974):

$$\delta^{13}\text{C}_{\text{CO}_2} = - \frac{C_T \delta^{13}\text{C}_{\text{DIC}} - [\text{H}_2\text{CO}_3^*](\varepsilon_{\text{CO}_2-\text{H}_2\text{CO}_3}) + [\text{HCO}_3^-](\varepsilon_{\text{CO}_2-\text{HCO}_3}) + [\text{CO}_3^{2-}](\varepsilon_{\text{CO}_2-\text{CO}_3^{2-}})}{[\text{H}_2\text{CO}_3^*]\alpha_0 + [\text{HCO}_3^-]\alpha_1 + [\text{CO}_3^{2-}]\alpha_2} \tag{1}$$

where, (H_2CO_3^*) = molality of dissolved CO_2 and carbonic acid (H_2CO_3), (HCO_3^-) = molality of bicarbonate ion; (CO_3^{2-}) = molality of the carbonate ion; C_T (total carbon) = (H_2CO_3^*) + (HCO_3^-) + (CO_3^{2-}); α_0 = fractionation coefficient of $\text{H}_2\text{CO}_3^*-\text{CO}_2$ (g) reaction; α_1 = fractionation coefficient of $\text{HCO}_3^--\text{CO}_2$ (g) reaction; α_2 = fractionation coefficient of $\text{CO}_3^{2-}-\text{CO}_2$ (g) reaction and represents the fractionation factor (% vs PDB) of the indicated species with gaseous CO_2 .

The $\delta^{13}\text{C}$ fractionation factor between DIC species and gaseous CO_2 is calculated using the following equations at isotope equilibrium (Vogel et al. 1970; Mook et al. 1974; Deines et al. 1974):

$$\begin{aligned} \varepsilon^{13}\text{C}_{\text{CO}_2(\text{aq})-\text{CO}_2(\text{g})} &= 10^3 \ln \alpha^{13}\text{C}_{\text{CO}_2(\text{aq})-\text{CO}_2(\text{g})} \\ &= -0.373(10^3 T^{-1}) + 0.19 \end{aligned} \tag{2}$$

$$\begin{aligned} \varepsilon^{13}\text{C}_{\text{HCO}_3-\text{CO}_2(\text{g})} &= 10^3 \ln \alpha^{13}\text{C}_{\text{HCO}_3-\text{CO}_2(\text{g})} \\ &= 9.552(10^3 T^{-1}) - 24.10 \end{aligned} \tag{3}$$

and

$$\begin{aligned} \varepsilon^{13}\text{C}_{\text{CO}_3-\text{CO}_2(\text{g})} &= 10^3 \ln \alpha^{13}\text{C}_{\text{CO}_3-\text{CO}_2(\text{g})} \\ &= 0.87(10^6 T^{-2}) - 3.4 \end{aligned} \tag{4}$$

Results

Physical parameters

In situ parameters such as pH, temperature and EC, together with analytical data for the major ions and isotopes in the groundwater samples, are presented in Table 1. The measured EC of all sampled water varies from 86 to 2,150 $\mu\text{S}/\text{cm}$. It is found that water samples taken from shallow wells, springs and rivers have low mean EC value ($<500 \mu\text{S}/\text{cm}$), whereas water samples taken from deep wells, hot springs and lakes have a mean EC value $>500 \mu\text{S}/\text{cm}$. The pH value ranges from slightly acidic to nearly alkaline (5.4–8.5) in groundwater wells, hot springs and river water, whereas the lake water has a pH in the range of 7–10.1. The measured temperature of all water samples ranges from 19 to 81 $^{\circ}\text{C}$. Some shallow wells (A8, A11, and A12) have anomalous groundwater temperatures of 38.7, 34.5 and 33.7 $^{\circ}\text{C}$, respectively, and the remaining shallow wells have a value of 21–26 $^{\circ}\text{C}$. Groundwater from deep wells has a temperature in the range of 19–40 $^{\circ}\text{C}$ with a mean value of 26.7 $^{\circ}\text{C}$. Deep wells A16, A21, A29, and A39 have anomalous temperatures of 34, 40, 31, and 33 $^{\circ}\text{C}$, respectively, while the rest of the deep wells are in the range of 19–29 $^{\circ}\text{C}$. All water samples from hot springs are characterized by a temperature of 35–81 $^{\circ}\text{C}$. The study has found that there is gradual increase of temperature, EC and pH from the highland to the rift floor.

Major ions

The relative distributions of dissolved major cations and anions show variability in the area. It is found that groundwater of the study area has Na^+ ions as the dominant cations, followed by calcium. High relative Na^+ content of groundwater is mostly associated with the deep aquifer, whereas high Ca^{2+} has prevailed in groundwater from the shallow aquifer. The impact of cation concentration is found more than with anion concentration in the groundwater. Ca^{2+} and Mg^{2+} are the dominant cations of groundwater in the highland, whereas Na^+ and K^+ are dominant cations of groundwater in the rift floor. Dissolved anions of the groundwater are strongly dominated by HCO_3^- , followed by Cl^- and SO_4^{2-} . Based on the obtained hydrochemical data, the groundwater samples are classified into different groups as: Ca-Mg- HCO_3 , Ca-Na- HCO_3 , Ca-Na-Mg- HCO_3 , Na-Ca-Mg- HCO_3 , Na-Ca- HCO_3 and Na- HCO_3 ; however, the dominant water types are Ca-Mg- HCO_3 , Na-Ca- HCO_3 and Na- HCO_3 .

Sulfate concentration ranges from 0.1 to 652 mg/L and chloride concentration ranges from 0.97 to 611 mg/L in all water samples (Table 1). There is a considerable amount of sulfate in hot springs and lakes, while chloride in some shallow wells and springs. NO_3^- concentration ranges from 0.20 to 73.9 mg/L for all water samples. The highest amount of NO_3^- content is

observed in deep wells, e.g. A35 and A40, with concentrations of 18.08 and 63.57 mg/L, respectively. Water samples from springs A47, A49 and A53 have NO_3^- concentrations of 19.84, 73.9 and 23.24 mg/L, respectively. There is also a large amount of NO_3^- in water from shallow wells such as A1, A6, and A9, with concentrations of 69.5, 24.9 and 27.9 mg/L, respectively. The F^- concentration ranges from 0.09 to 57.4 mg/L for all water samples. In the shallow aquifers, the F^- concentration varied between 0.09 and 1.51 mg/L with a mean value of 0.78 mg/L. All groundwater from shallow wells had F^- concentrations below 1.5 mg/L (WHO drinking-water quality guidelines) except A2 which has a value of 1.51 mg/L. Groundwater samples from the deep aquifers had F^- concentrations ranges from 0.48 to 5.61 mg/L. It is found that more than 70% of the deep groundwater has F^- concentrations in excess of the WHO standard for drinking water (1.5 mg/L) and are mainly located around the town of Halaba. One water sample (A52) collected from a spring around the town of Bodity contained 1.66 mg/L of F^- , whereas elevated F^- concentration was also observed in all hot springs, up to 57.39 mg/L (A56).

$\delta^{18}\text{O}$ and δD

The isotopic ratios of $\delta^{18}\text{O}$ and δD of groundwater and surface water from Abaya Chamo basin are presented in Fig. 2 along with the Global Meteoric Water Line (GMWL), the Addis Ababa Meteoric Water Line (AAMWL) and the mean weighted summer rain at Addis Ababa station ($\delta^{18}\text{O} = -2.56\text{‰}$). It appears that all the groundwater samples plot close to the AAMWL. The $\delta^{18}\text{O}$ and δD values of surface water (rivers and lakes) range from about -2.9 to 8‰ and -4.9 to 51‰ , respectively. It is observed that lake water samples plot below the GMWL and the AAMWL on a regression line (LEL; $\delta\text{D} = 4.84\delta^{18}\text{O} + 8.54$). On the other hand, groundwater samples show a range of -4.9 to -1.1‰ for $\delta^{18}\text{O}$ and -27 to 5.3‰ for δD . Based on the obtained isotopic ratios, two groups of groundwater in the Abaya Chamo basin were identified. Group I is enriched with $\delta^{18}\text{O}$ value of -0.8 to -3.4‰ VSMOW and δD value of 11.6 to -12.7‰ VSMOW, which are identified in the water samples collected from shallow wells, deep wells, cold springs, and hot springs. Group II is depleted, with $\delta^{18}\text{O}$ values of -3.8 to -4.9‰ VSMOW and δD value of -18 to -27‰ VSMOW. The $\delta^{18}\text{O}$ values are found even lower than the average summer $\delta^{18}\text{O}$ value of Ethiopian rainfall, which are identified in the water samples collected from deep wells in the town of Halaba and surrounding villages northeast of the study area.

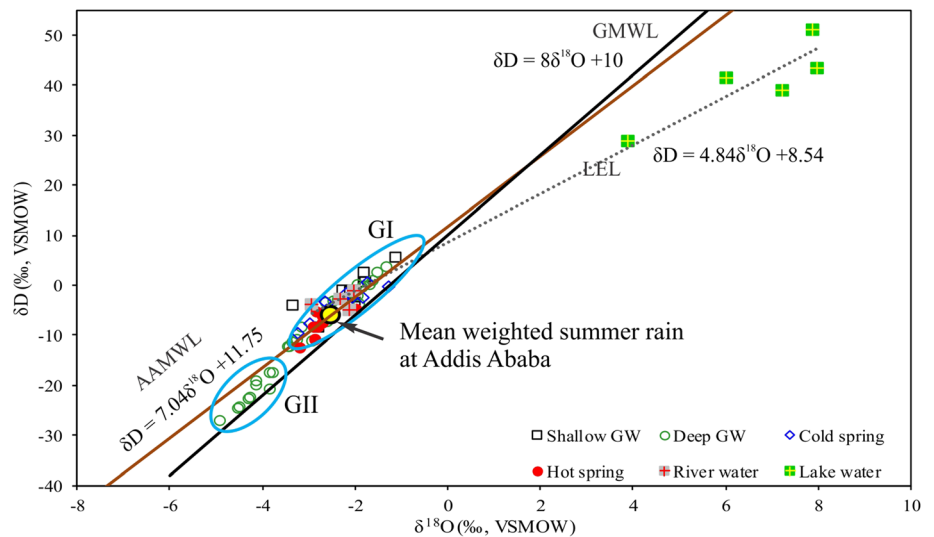
$\delta^{13}\text{C}_{\text{DIC}}$

$\delta^{13}\text{C}_{\text{DIC}}$ values of all water samples range from -12.0 to $+1.6\text{‰}$ (VPDB; Table 1). Groundwater samples from shallow wells and cold springs show a depleted composition of $\delta^{13}\text{C}_{\text{DIC}}$ in the range of -6.7 to -12‰ ; however, groundwater

Table 1 Summary of chemical and isotope measurements of water samples from the volcanic aquifer of Abaya Chamo basin

Source type	Shallow groundwater (n=13)			Deep groundwater (n=31)			Cold springs (n=11)			Hot springs (n=8)			River water (n=3)			Lake water (n=5)		
	Min	Max	Mean	Min	Max	Mean	Min	Max	Mean	Min	Max	Mean	Min	Max	Mean	Min	Max	Mean
Temperature (°C)	21.0	38.7	25.7	19.5	40.6	26.9	19.0	32.8	23.7	35.8	81.0	51.2	19.5	24.7	22.7	23.6	28.5	26.5
pH	5.4	8.0	–	6.1	8.2	–	5.6	7.8	–	6.4	8.5	–	7.4	8.5	–	6.9	10.1	–
EC (µS/cm)	112.1	767.0	440.1	151.4	939.0	535.3	94.0	633.0	256.4	405.0	2,150.0	1,355.9	86	219	154.3	187.0	26,300	9,684.2
Na ⁺ (mg/L)	7.8	52.7	29.5	7.0	106.0	40.37	5.7	40.8	19.9	37.4	544.7	159.0	4.4	17.0	9.4	15	4,250	2,047.1
K ⁺ (mg/L)	0.5	16.8	6.6	0.5	19.0	9.44	1.5	12.8	6.2	9.8	39.7	25.9	0.9	7.2	3.03	12.8	282	103.9
Mg ²⁺ (mg/L)	0.6	25.8	10.5	0.2	35.9	11.9	0.9	22.2	5.6	0.3	49.7	15.2	2.8	6.4	4.7	0.5	4.3	2.2
Ca ²⁺ (mg/L)	2.0	48.3	25.6	1.4	76.3	28.2	3.5	31.3	13.2	3.5	42.4	20.1	6.1	12.2	9.9	2.4	17.6	9.5
Cl ⁻ (mg/L)	0.9	35.1	12.1	1.1	71.6	7.9	1.8	34.2	8.3	3.4	93.2	51.7	1.2	3.6	2.1	11.4	611.4	257.1
SO ₄ ²⁻ (mg/L)	0.4	74.9	8.7	0.0	18.3	4.7	0.5	6.9	1.9	0.8	106.0	26.9	0	12.8	4.6	1	611.4	257.1
HCO ₃ ⁻ (mg/L)	26.8	411.9	201.4	99.2	442.4	249.7	40.3	358.5	116.8	167.8	1167	596.1	83.5	246.7	141.4	37.1	4,114	1,796.1
NO ₃ ⁻ (mg/L)	0.0	69.5	12.5	0.0	63.6	5.5	0.7	73.9	13.5	0.7	8.9	2.11	0	2.12	1.1	1.2	42	9.9
F ⁻ (mg/L)	0.1	1.5	0.6	0.2	5.6	1.8	0.2	1.7	0.6	1.5	57.4	16.6	0.0	0.6	0.3	0.2	112	41.4
δ ¹⁸ O (‰ VSMOW)	-3.4	-1.1	-2.1	-4.9	-1.3	-2.9	-3.2	-1.3	-2.3	-3.2	-2.0	-2.7	-2.9	-2.0	-2.4	3.9	7.9	6.6
δD (‰ VSMOW)	-8.5	5.3	-1.5	-30.9	3.7	-9.8	-9.7	0.4	-3.4	-12.7	-4.8	-8.1	-3.7	-1.1	-2.5	28.8	51.1	40.7
δ ¹³ C (‰ VPDB)	-11.8	-1.5	-7.3	-10.9	-2.7	-6.6	-11.1	-7.6	-9.1	-8.3	1.6	-1.3	-7.9	1.2	-3.4			
δ ¹³ CCO ₂ (‰ VPDB)	-19.4	-7.7	-13.9	-18.6	-10.1	-13.5	-18.9	-9.2	-14.2	-11.6	-0.8	-5.6						

Fig. 2 Plot of $\delta^{18}\text{O}$ and δD values of Abaya Chamo basin water samples. GMWL: Global Meteoric Water Line, AAMWL: Addis Ababa Local Meteoric Water Line, LEL: local evaporation line, and GW: groundwater



samples from two shallow wells (A4 and A5) have a value of -2.2 and -1.5‰ , respectively. Groundwater from the deep wells has a wide range of $\delta^{13}\text{C}$ values (-2.7 to -10.9‰). All water samples from hot springs are enriched in $\delta^{13}\text{C}$ and have a narrow range (-2.3 – 1.6‰), except A63 which has a value of -8.3‰ . $\delta^{13}\text{C}_{\text{DIC}}$ shows an increasing trend with the increase of DIC concentration; in particular, there is a strong correlation at high DIC (>6 mmol/L) and high $\delta^{13}\text{C}$ ($> -4\text{‰}$) as shown in Fig. 3a, which is related to the evolutionary trend existing between rising pH and increasing HCO_3^- content as shown in Fig. 3b. Water samples from cold springs show low pH and HCO_3^- , as well as a depleted $\delta^{13}\text{C}$ signature, whereas, groundwater samples from the rift floor and hot springs have higher pH and HCO_3^- and show a more enriched $\delta^{13}\text{C}$ signature. The highest $\delta^{13}\text{C}$ enrichment was measured in thermal groundwater originating from the northern part of Lake Abaya area (Abaya geothermal field). Also, the samples of thermal groundwater display the highest HCO_3^- concentrations.

Discussion

Groundwater chemical composition and its spatial variation

Groundwater samples from the Abaya Chamo basin show a clear spatial hydrochemical distribution. There are distinct differences in hydrochemistry found between the highlands and the Rift Valley, and between the deep and shallow aquifer systems, as shown in Fig. 4b. Groundwater samples that were collected from the western part of the Lake Abaya area are predominantly Ca-Mg- HCO_3 type, whereas groundwater samples that were collected from the northwestern part of the area are predominantly Na- HCO_3 type. In 17.1% of the total water samples, it is observed that hydrochemical facies are dominated by Ca-Mg- HCO_3 with the mean value of EC being $400 \mu\text{S}/\text{cm}$. These characteristics are associated with the shallow system, in which circulation occurs in the basaltic and alluvial aquifers

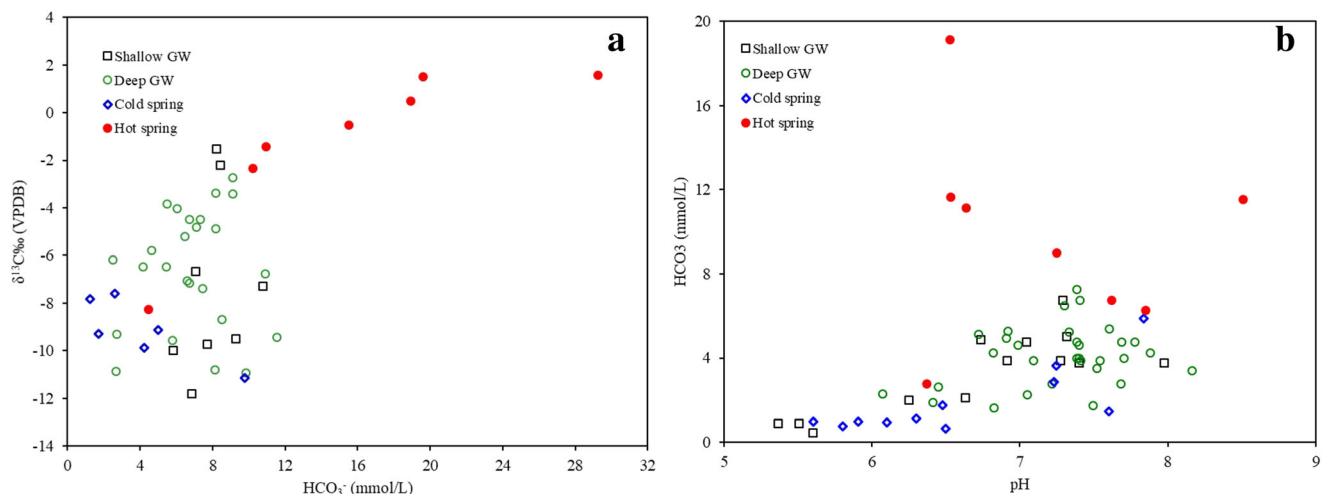


Fig. 3 Relationships between **a** stable carbon isotopes ($\delta^{13}\text{C}_{\text{DIC}}$) with DIC of the water and **b** pH and HCO_3^- of sampled groundwater

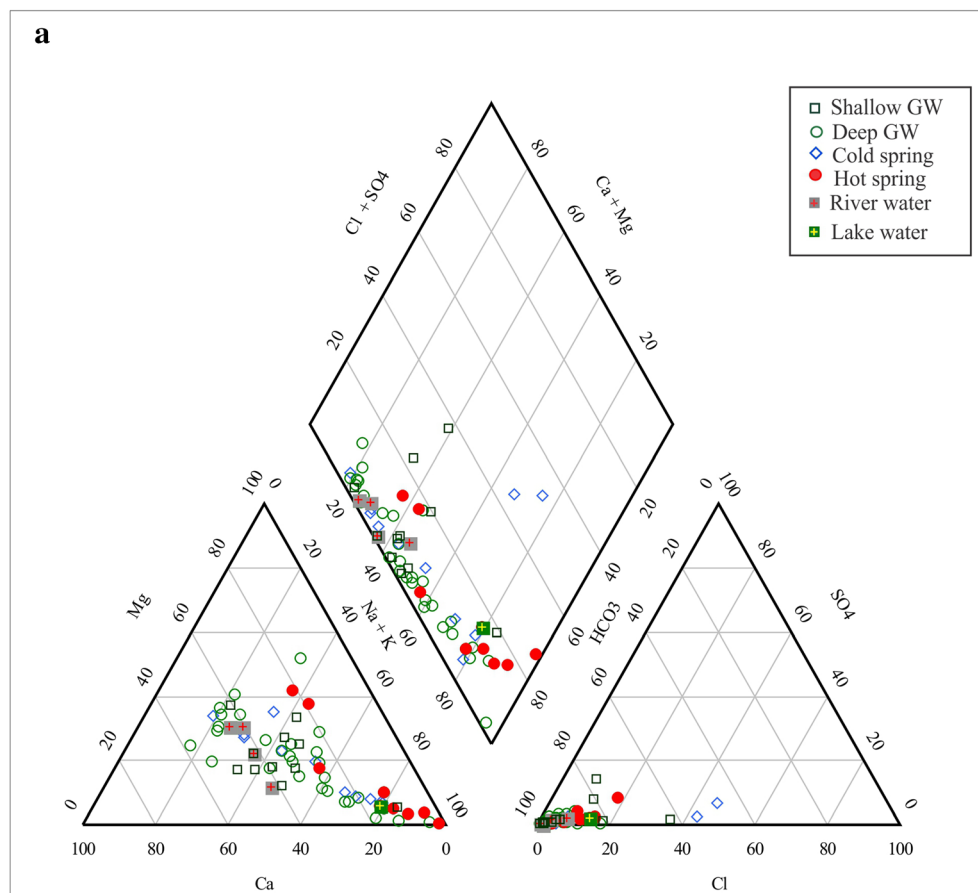


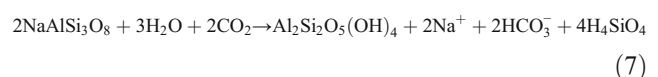
Fig. 4 **a** Piper diagram and **b** map showing the spatial distribution of hydrochemical facies and $\delta^{18}\text{O}$ content of groundwater in the basin. Note: the legend for colored areas of the background map is given in Fig. 1

that are mainly distributed in the highland part of the study area. Ca-Mg-HCO₃ water types are most probably a result of interaction with basaltic rocks and alluvial deposits where the main composition of basalt is Ca and Mg. Ca-Mg-HCO₃ and Ca-HCO₃ groups represent groundwater either at the early stages of geochemical evolution (recent recharge) or within a system of rapidly circulating groundwater (Adams et al. 2001; Kebede et al. 2005; Marini et al. 2000). Hydrochemical facies dominated by Ca-Na-HCO₃ with EC ~420 $\mu\text{S}/\text{cm}$ are mainly distributed in the escarpment of the study area, which is characterized by intercalations of acidic volcanic rocks. These characteristics relate to 15.8% of the total water samples. The interaction that occurs between groundwater and weathered and fractured rocks rich in Ca- and Na-plagioclases leads to the formation of Ca-Na-HCO₃ type water. The other facies groups constitute Na-Ca-HCO₃ and Na-HCO₃ water types, which are mainly encountered in the northwestern part of the study area. These two hydrochemical facies are found in 67.1% of the total water samples. Groundwater from deep wells show Na-Ca-HCO₃/Na-HCO₃ water type with an increase in EC (mean ~560 $\mu\text{S}/\text{cm}$) pointing to longer residence times and increased water-rock interaction.

Geochemical processes controlling groundwater chemistry

Different geochemical processes occur during rock–water interaction, which include dissolution/precipitation, ion exchange, hydrolysis, oxidation and reduction (Elango and Kannan 2007; Li et al. 2015). The hydrolysis of silicate rocks is a key geochemical process, which controls the major ions of the groundwater chemistry and results in the release of Ca²⁺, Mg²⁺, K⁺ and Na⁺ and HCO₃⁻ into the groundwater (Appelo and Postma 2005; Clark 2015).

Silicate minerals are the main component of the volcanic rock aquifers in the study area. The hydrolysis of silicate is controlled by the uptake of CO₂ in the study area (Darling et al. 1996). The bicarbonate content is found to be related to concentrations of dissolved cations, as in the following reactions given:



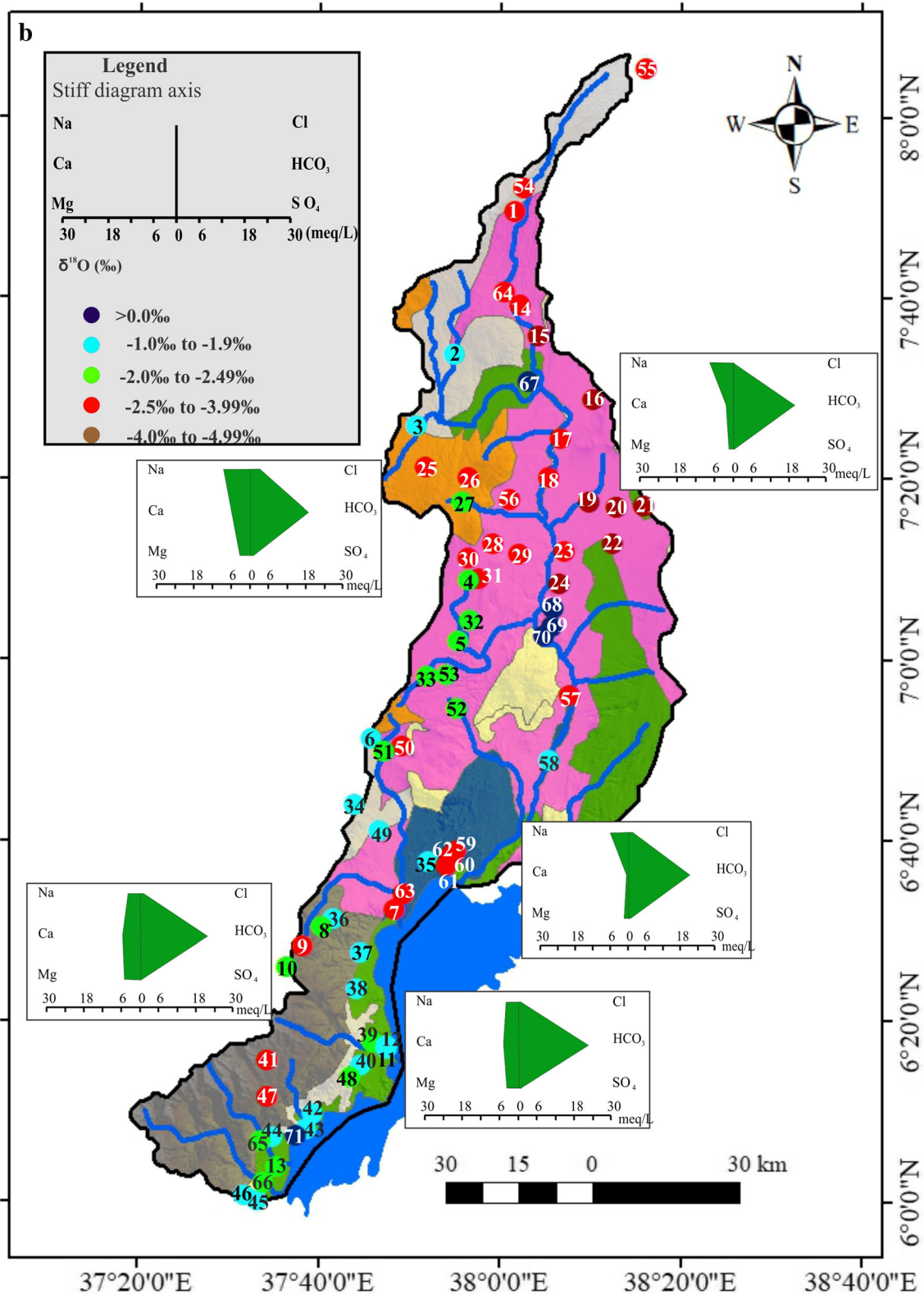


Fig. 4 (continued)

The correlation of cationic species [Ca²⁺ + K⁺ + Mg²⁺ + Na⁺] and [HCO₃⁻] suggests that the cations are balanced

mainly by the bicarbonate anion as shown in Fig. 5a. Similarly, the relationship between Ca²⁺ + Mg²⁺ and HCO₃⁻

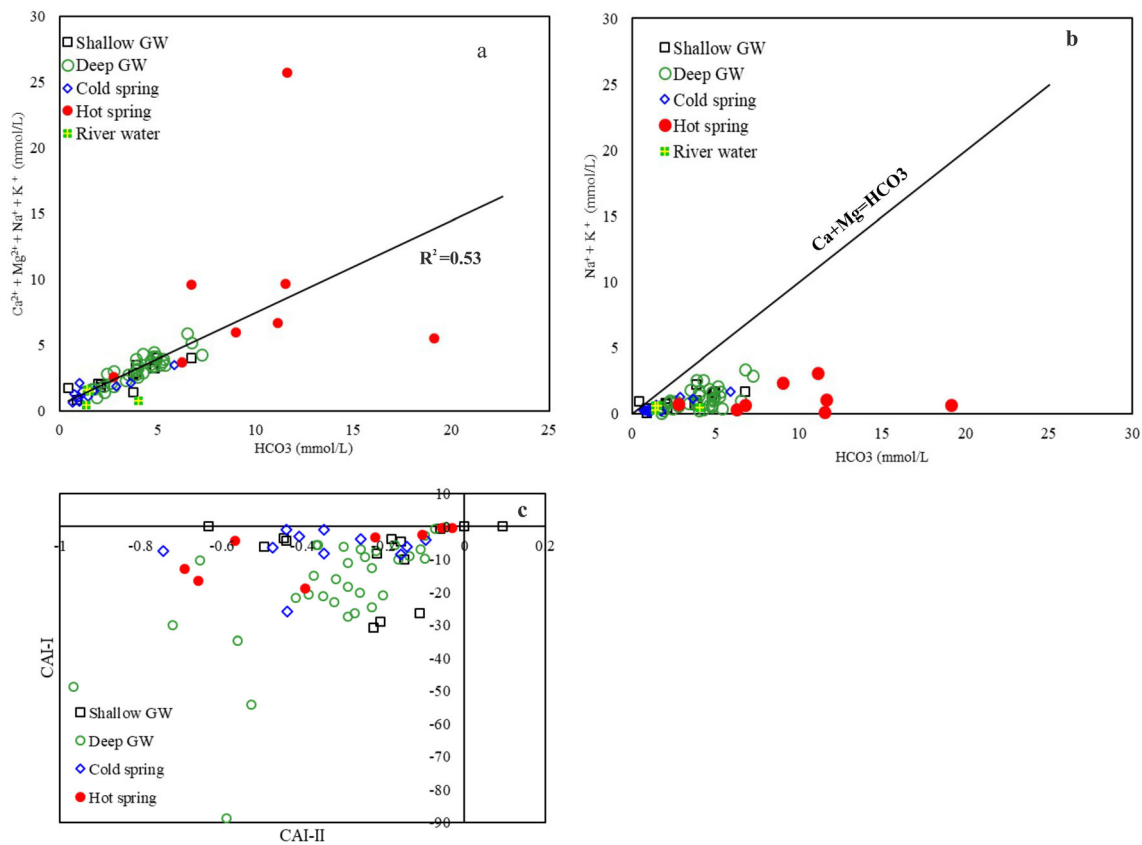


Fig. 5 a Plot of $(Ca^{2+} + K^{+} + Mg^{2+} + Na^{+})$ and (HCO_3^{-}) , b plot of $(Ca^{2+} + Mg^{2+})$ and (HCO_3^{-}) and c plot of CAI-II vs. CAI-I

helps to distinguish between carbonate weathering and silicate weathering. The ionic concentration falling above the equiline occurs due to carbonate weathering, whereas ionic concentration falling below the equiline occurs due to silicate weathering and the dominance of HCO_3^{-} over Ca^{2+} and Mg^{2+} (Elango et al. 2003). The plot of $Ca^{2+} + Mg^{2+}$ vs. HCO_3^{-} shows that all water samples fall below the 1:1 line as shown in Fig. 5b. The relationships obtained from the two plots suggests that silicate hydrolysis is the most governing hydrochemical process and the main source of these ions in the groundwater. Thus, this process has increased the cationic concentration and bicarbonate ion contents in the groundwater of the study area.

The cationic exchange between Na^{+} and Ca^{2+} is an important natural process with significant influences on groundwater chemistry. The two chloro-alkaline indices CAI-I and CAI-II were used to investigate the occurrence of cation exchange reactions in this area as suggested by Shoeller (1967). These two indices are expressed as Eqs. (8) and (9) (all ions are expressed in meq/L).

$$CAI-I = \frac{[Cl-(Na + K)]}{Cl} \quad (8)$$

$$CAI-II = \frac{[Cl-(Na + K)]}{SO_4 + HCO_3 + CO_3 + NO_3} \quad (9)$$

As shown in Fig. 5c, nearly all groundwater samples resulted in negative values for both indices. This clearly indicates that cation exchange takes place between Ca^{2+} in the water and Na^{+} in the aquifer material. The outcome shows that shallow groundwater and cold water springs appear scattered in the narrow range for CAI-I and CAI-II, while deep groundwater of the Abaya Chamo lakes basin reveals a very wide variation in these two indices, as shown in Fig. 5c. From the obtained results, it is inferred that deep groundwater was affected by various degrees of the cation exchange process. The cation exchange also resulted in the high Na^{+}/Ca^{2+} ratio of deep groundwater in the rift floor (0.44–12.37) compared to that in the shallow groundwater (1.02–4.13) of the highland and escarpment. This clearly indicates that there is an increase in cation exchange in the central basin, where significantly elevated Na^{+}/Ca^{2+} ratios and sodium contents are observed.

Mineral stability diagrams were used to assess groundwater–rock equilibrium. In order to study the equilibrium of groundwater with silicate, mineral balance diagrams of $K^{+}-H^{+}-SiO_2$, $Na^{+}-H^{+}-SiO_2$ and $Ca^{2+}-H^{+}-SiO_2$ were employed (Fig. 6a–c). The obtained results show that all samples lie within the kaolinite and montmorillonite stability field. Almost all the samples plotted within the montmorillonite field belong to the deep groundwater and hot springs, while those plotted in the kaolinite field of stability are mainly from

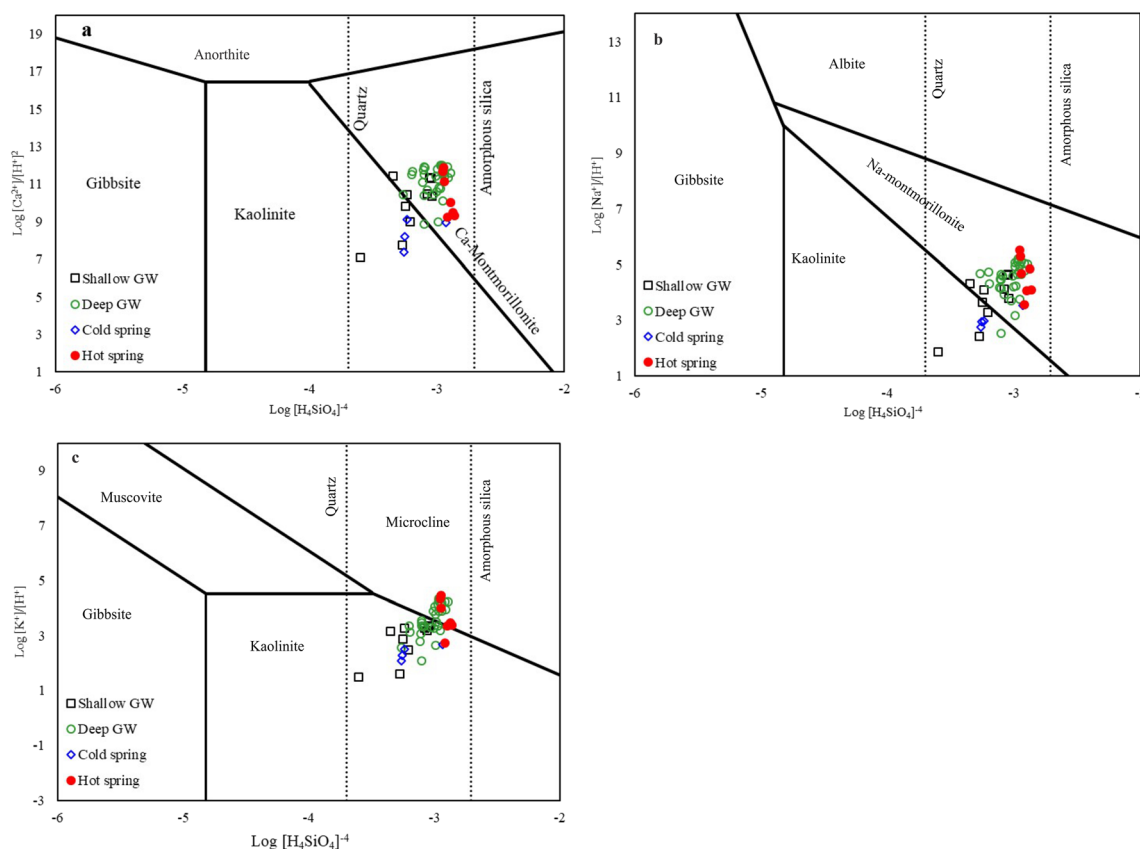


Fig. 6 Stability phase diagrams for **a** CaO-Al₂O₃-SiO₂-H₂O, **b** Na₂O-Al₂O₃-SiO₂-H₂O and **c** K₂O-Al₂O₃-SiO₂-H₂O systems, together with the chemical compositions of the sampled water from Abaya Chamo area. Solubility constants from Tardy (1971) were used for construction (25 °C and 1 atm)

shallow groundwater and cold springs. This clearly indicates the existence of two different flow systems; thus, the dissolution of primary silicates like plagioclase is an ongoing process to form secondary silicates like kaolinite and montmorillonite. On the other hand, kaolinite and montmorillonite clay minerals act as exchange media for cations. Reactions involving dissolution-precipitation of volcanic rock, as well as adsorption and ion exchange related to clay minerals, significantly influence the change in major ion composition of the groundwater; hence, this resulted in the high concentration of ions that are observed in groundwater of the deep aquifer (e.g. Na⁺, HCO₃⁻ and F⁻, see Table 1).

Origin and circulation of groundwater

The isotopic compositions ($\delta^{18}\text{O}$ and δD) of the groundwater samples are distributed around the mean summer $\delta^{18}\text{O}$ and δD composition of the Ethiopian rainfall. The mean weighted value of $\delta^{18}\text{O}$ of summer precipitation at Addis Ababa obtained from the International Atomic Energy Agency (IAEA) records is -2.56‰ . In the Abaya Chamo basin, the isotopic composition of groundwater ($\delta^{18}\text{O}$ and δD) very well represents the average isotopic composition of Ethiopian summer rainfall as recorded at the Addis Ababa IAEA station. The

similarity of $\delta^{18}\text{O}$ content between groundwater and summer rainfall indicates that the recharge occurs mainly from summer rainfall.

The isotopic signature of the groundwater samples shows a spatial variability across the study area as shown in Fig. 4b. From the highland to the rift floor, except in hot springs, there is a general progressive enrichment in the $\delta^{18}\text{O}$ and δD values of groundwater in the western part of Lake Abaya area. This trend suggests the importance of evaporative fractionation before the process of recharge and the percolation of shallow groundwater into deep aquifers. It is observed that there are high amounts of NO₃⁻ coupled with high Cl⁻ content in the western lowland groundwater of Lake Abaya area, and this is evident from the analytical results of water samples A35, A40, and A44. The observed high content of NO₃⁻ indicates percolation of shallow groundwater into the deep aquifer.

The variation that occurs in the values of $\delta^{18}\text{O}$ and δD in all hot springs does not fit into the progressive enrichment trend. Depletion of $\delta^{18}\text{O}$ and δD content occurs in the hot spring waters, and these samples also show similar values to that of the groundwater in the highland of the western part, which indicates that the main source of recharge of the thermal water is the groundwater from the highland. Also, cold shallow groundwater in the lowland of western Lake Abaya and the

cold deep groundwater in the highlands show similar $\delta^{18}\text{O}$ values. This suggests that the groundwater inflow from the mountains is the principal source of recharge in the rift plain of the western Lake Abaya area, in addition to sporadic rainfall recharge. In general, there is similarity in the stable isotopic compositions of shallow groundwater, deep groundwater, rivers and rainwater, suggesting a good hydrological connection in the study area, particularly at the western part of Lake Abaya area.

Groundwater in the area of the northern part of Lake Abaya shows progressive depletion of $\delta^{18}\text{O}$ from the highland to the rift floor, as shown in Fig. 4b. The depletion of $\delta^{18}\text{O}$ in groundwater in this part is also accompanied by increasing trends in EC , F^- and HCO_3^- . The successive accumulation of ions and depletion of $\delta^{18}\text{O}$ is indicative of deep groundwater flow and long residence time. Groundwater samples such as A19, A20, A21, A22, and A24, were taken from the deep wells located in the northeast of the town of Halaba, and these show strong depletion in $\delta^{18}\text{O}$ and δD with respect to modern rainfall and other groundwater samples of the area. Such strong depletion of the deep groundwater occurs due to an altitude effect or a climatic effect. Assuming conservative behavior of the stable oxygen isotope (Clark and Fritz 1997), the relationship between $\delta^{18}\text{O}$ values and altitude was established (Fig. 7). The analysis of cold spring data indicates that there is a decrease in $\delta^{18}\text{O}$ of 0.09‰ per 100 m rise in elevation, which is similar to the -0.1‰ shift per 100 m rise in elevation reported by (Kebede et al. 2005) for the northwestern Ethiopian Plateau. Taking into account the relationship of $\delta^{18}\text{O}$ and altitude of $-0.09\text{‰}/100\text{ m}$, the mean recharge altitude for such depleted groundwater is calculated to be 3,700 m above sea level (asl); however, the main surrounding reliefs reach, at most, an altitude close to 3,500 m asl. Hence, no matching is found between the estimated altitudes of the potential recharge areas and the elevation of the aquifer recharged in the study area; therefore, the altitude effect is

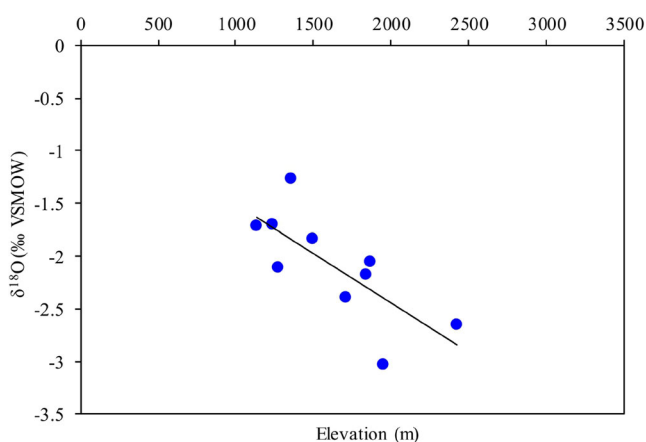


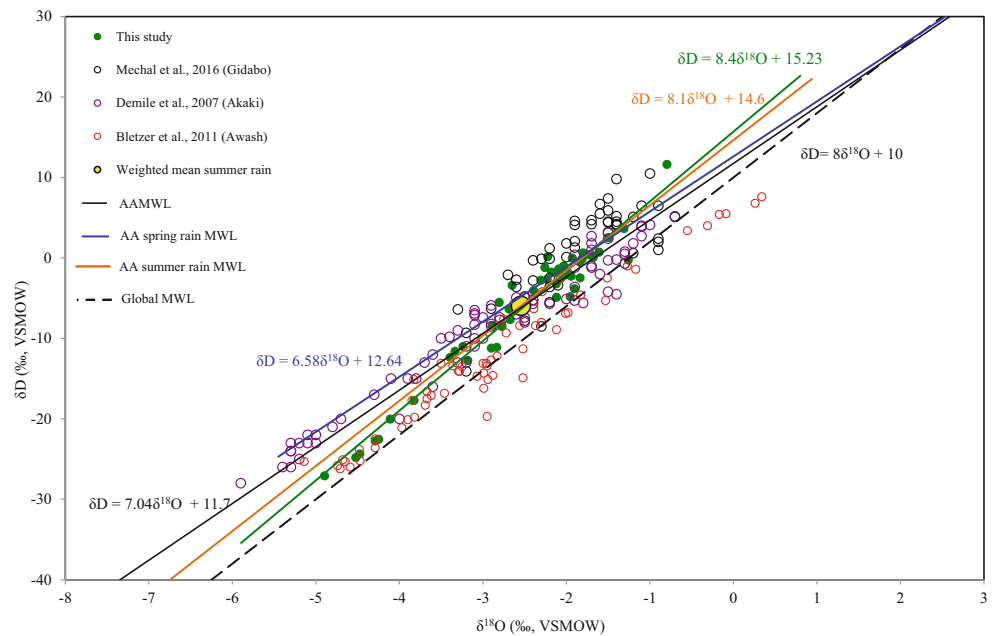
Fig. 7 Cold spring $\delta^{18}\text{O}$ vs elevation. The linear trend shows an isotopic gradient of -0.09‰ per 100 m rise of elevation in meters: $\delta^{18}\text{O} = -0.0009 \times \text{elevation} - 0.6422$ ($R^2 = 0.74$)

not responsible for this depletion. It is likely that the occurrence of depleted isotopes in groundwater can be attributed to a deeper aquifer that was recharged under different (e.g. colder) climatic conditions with respect to the present day, thereby justifying the isotopic values obtained. This is in accord with depletion of stable isotopes caused by climatic change as recorded in lake sediments (Lamb et al. 2007).

Isotopic signal of groundwater recharge

Using groundwater samples as a basis of comparison, Fig. 8 compares the $\delta^{18}\text{O}$ compositions of the southern Main Ethiopian Rift (Abaya Chamo basin and Gidabo River basin) with that of the northern Main Ethiopian Rift (upper and middle Awash River basin) and western margin of the Main Ethiopian Rift (Akaki River catchment). The spatial variation of isotopes reflects the climate differences of the regions. Groundwaters of the Abaya Chamo basin, Gidabo River basin and Akaki catchment plot above the GMWL and they have the highest d-excess. It is found that groundwaters of Awash River basin plot below the LMWL and to some extent below the GMWL. The obtained data indicate that the groundwater undergoes a process of recharge from local modern rainfall, whereas those points that plot below the LMWL and GMWL show that the groundwater undergoes a clear evaporative fractionation prior to recharge. The isotopic compositions of the groundwater samples of Abaya Chamo basin and Gidabo River basin follow a line defined by the dataset of the nonevaporated summer rains at Addis Ababa, whereas the groundwater samples of Akaki River catchment plot above or below the LMWL defined by the entire record dataset of monthly rains at Addis Ababa. Groundwater from the upper and middle Awash River basin plot below the LMWL defined by the entire record dataset of monthly rains at Addis Ababa. The stable isotope composition of water is essentially conservative at ambient temperatures during passage within the aquifer. The proximity of the dataset to different trend lines can be explained by the importance of rainfall recharge to the aquifer. If recharge conditions derive totally from the recorded rain of all time, groundwater should follow a line parallel to the one defined by the monthly rain at Addis Ababa; however, groundwater from the western ACB rather follows a line that defines summer rain at Addis Ababa. Meanwhile, the $\delta^{18}\text{O}$ and δD plots for southern Ethiopia's groundwater (western ACB) fall along a trend line with an R^2 value of 0.95 and the equation of $\delta\text{D} = 8.7 \delta^{18}\text{O} + 15.7$, which is very similar to the summer LMWL ($\delta\text{D} = 8.1 \delta^{18}\text{O} + 14.6$). This suggests that groundwater recharges mainly from summer rainfall in southern Ethiopia, and the isotopic composition of heavy rainfall events appears to be a better indicator of the input isotopic signal for groundwater. This highlights the necessity to consider changing rainfall intensities in the assessment of climate-change impacts on groundwater recharge in southern Ethiopia.

Fig. 8 Plot of the $\delta^{18}\text{O}$ and δD values of groundwater of western Abaya Chamo basin water, Gidabo River basin, Akaki River catchment and Awash River basin



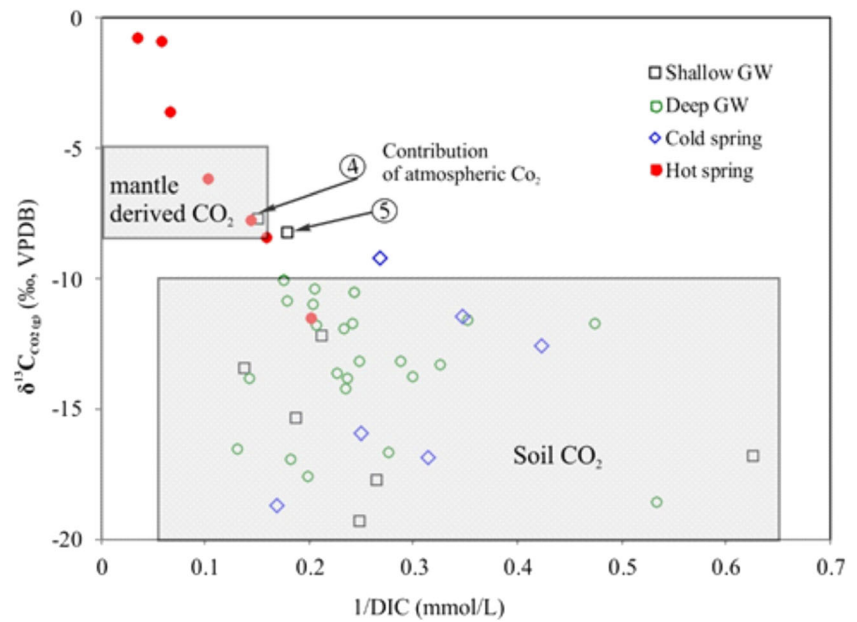
Source of $\delta^{13}\text{C}_{\text{DIC}}$ and its significance with respect to the groundwater flow system

The wide range of $\delta^{13}\text{C}_{\text{DIC}}$ in groundwater reflects multiple carbon sources, which also accounts for the higher P_{CO_2} (partial pressure of carbon dioxide) of groundwater. The $\delta^{13}\text{C}_{\text{DIC}}$ value shows that groundwater is likely to include magmatic CO_2 where such a wide range of $\delta^{13}\text{C}_{\text{DIC}}$ could not be accounted for by biogenic CO_2 from the soil zone. The calculated $\delta^{13}\text{C}_{\text{CO}_2}$ values range from -19.4 to -0.80‰ (see Table 1) and display a marked dependency on dissolved carbon concentrations, as shown in Fig. 9. This clearly indicates varying levels of geochemical evolution, different carbon sources and the existence of different flow systems. The water samples from the shallow wells and deep wells have $\delta^{13}\text{C}_{\text{CO}_2}$ values in the range of -19 to -8‰ , whereas the water samples of hot springs have $\delta^{13}\text{C}_{\text{CO}_2}$ values in the range of -1‰ to -11‰ (VPDB). The calculated $\delta^{13}\text{C}_{\text{CO}_2(\text{g})}$ values of water samples from shallow wells and cold springs range from -11.4 to -19.4‰ which overlap within the range of soil CO_2 . This indicates that the DIC is mainly derived from the soil zone of C3 and C4 plants. The $\delta^{13}\text{C}$ value range of soil dominated by C3 plants is -27 to -23‰ and the $\delta^{13}\text{C}$ values of soil dominated by C4 plants is between about -10 and -14‰ (Cerling and Harris 1999; Clark 2015). The values of $\delta^{13}\text{C}_{\text{CO}_2(\text{g})}$ are higher than those of biogenic CO_2 in the water samples of shallow wells A4 and A5, which could be due to the presence of some atmospheric CO_2 . At present, the $\delta^{13}\text{C}$ value of atmospheric CO_2 is about -8‰ (Clark 2015).

The $\delta^{13}\text{C}_{\text{CO}_2(\text{g})}$ values of groundwater samples taken from deep wells, with the range of -10 to -19‰ , show the intake of a typical soil carbon source by C3 and C4 plants and it is evident in the observed $\delta^{13}\text{C}_{\text{DIC}}$ values. However, high temperature, F^- and EC and heavier $\delta^{13}\text{C}_{\text{CO}_2(\text{g})}$ content are found in the groundwater samples of A19, A20, A21, and A22, taken from deep wells. This clearly indicates the occurrence of strong water–rock interaction, long residence time and lack of mixing with water from other sources. The highest enrichment of $\delta^{13}\text{C}$ was observed in hot springs originating from the northern Lake Abaya geothermal field. Similarly, the highest EC and HCO_3^- concentrations were observed in samples of the thermal water of the study area. The observed elevated HCO_3^- concentrations are attributed to another carbon dioxide source which reacts with the rock matrix and hence produces DIC. The obtained values of $\delta^{13}\text{C}_{\text{CO}_2}$ for these samples are in the range of -0.8 to -8‰ . Such a value of $\delta^{13}\text{C}$ indicates that, beside soil CO_2 , magmatic carbon may be an additional CO_2 source. The typical $\delta^{13}\text{C}$ values of CO_2 from magmatic origin range from -8 to -5‰ (e.g. Hoefs 2009) and the isotopic fractionation between CO_2 in magma and CO_2 gas can enrich gaseous CO_2 by about 2‰ . Accordingly, the value of $\delta^{13}\text{C}_{\text{CO}_2}$ in the hot springs is in general agreement with the isotopic composition of CO_2 from the magmatic origin.

The spatial distribution of $\delta^{18}\text{O}$, $\delta^{13}\text{C}$ and hydrochemical variation in the basin suggests that different flow systems exist. As shown in Fig. 10, the difference in the spatial distribution of $\delta^{18}\text{O}$ and δD , and the correlation between $\delta^{18}\text{O}$ and $\delta^{13}\text{C}$, clearly indicates that there is a slow movement of

Fig. 9 The $\delta^{13}\text{C}_{\text{CO}_2(\text{g})}$ of groundwater vs 1/DIC



groundwater through the volcanic aquifer in the northern part of the study area. Lighter $\delta^{18}\text{O}$ -bearing water is expected to have heavier $\delta^{13}\text{C}$ values, particularly for groundwater with long residence time, reaction with the aquifer matrix and lack of significant mixing with water of a different source. Similarly, heavier $\delta^{18}\text{O}$ -bearing water is expected to have lighter $\delta^{13}\text{C}$ values that are affected by soil carbon dioxide during shallow recharge. Groundwater in the northern part is probably hydraulically compartmentalized because of occurrences of barrier faults. In addition to barrier faults, volcanic rocks do not form extended aquifers and have deep static groundwater levels, to 294 m depth—for example, groundwater $\delta^{18}\text{O}$ and $\delta^{13}\text{C}$ values of closely spaced wells lying at similar water-level elevations are different, suggesting possible lack of hydraulic connection. There are also differences in the isotopic and chemical compositions of groundwater to the west and east of the Bilattie River. However, in the western

part of Lake Abaya area, due to the intense fracturing of rocks, it is assumed that there is a connection between shallow and deep circulating groundwater. In order to verify the connection between two systems, $\delta^{18}\text{O}$ versus $\delta^{13}\text{C}$ were plotted, as shown in Fig. 10. Samples with label GII were collected from the northern part and samples with label GI were collected from the western part of Lake Abaya area. In the absence of connection, the deep groundwater samples are expected to differ from shallow groundwater samples with respect to $\delta^{18}\text{O}$ and $\delta^{13}\text{C}$ signatures; however, the plot shows that the $\delta^{18}\text{O}$ and $\delta^{13}\text{C}$ values of deep groundwater samples are similar to those of shallow groundwater and cold spring water. This shows the existence of connection between the deep groundwater and the shallow groundwater within the rift floor.

Conceptual hydrogeological model of the area

Based on the groundwater geochemistry, isotopic compositions, and the lithological and geological structure, a conceptual model was established that shows the patterns of groundwater circulation and evolution in Abaya Chamo Basin. Weathered and fractured basalts and ignimbrites are the major aquifers in the highland and escarpment, whereas the main aquifers in the rift floor are composed of a mixture of pyroclastic flows (ignimbrite and pumice) or alluvial and lacustrine deposits. The area comprises a series of NNE–SSW trending horst and graben structures and normal faults running parallel and subparallel to the NE–SW trending main rift axis. Recharge mainly takes place in the mountains and upper escarpment and gradually drops towards the center of the rift floor due to the decreasing rainfall rate. The combination of steep slope and geological features (highly fractured and weathered volcanic rocks) favor the infiltration of water in

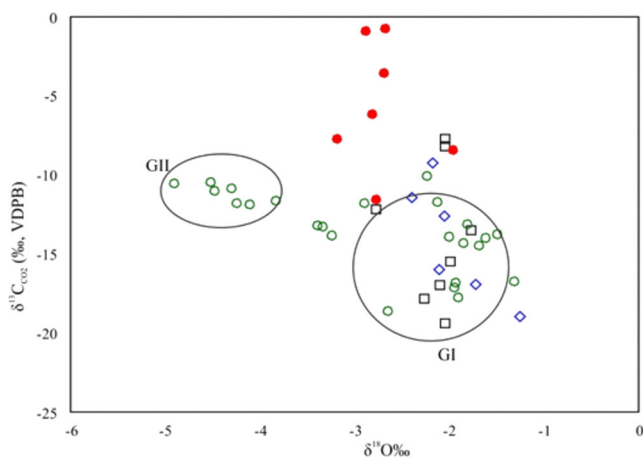


Fig. 10 Plot of $\delta^{13}\text{C}$ of gaseous carbon dioxide of water vs $\delta^{18}\text{O}$

the highland. The difference in topography and elevation between the highlands and the rift floor favor the formation of local and deep flow systems. Small local ridges on the rift floor generate a shallow groundwater flow system and create local groundwater divides that conform to the surface-water divides. In the highland and escarpment, parts of the water recharged to the shallow groundwater flow system discharge to the nearby depressions contributing to the base flow of streams and springs. The remaining water moves to the deep groundwater flow system that is directed towards the rift floor as shown in Fig. 11. Groundwater flow is controlled by a series of normal faults mainly oriented parallel and subparallel to the NE–SW trending rift axis. This is clearly seen by progressive increase in spring discharge from the highland to the rift floor and the existence of wetlands and swamps, and

suggests that the faults have a role in the occurrence of springs and in draining groundwater from the highland to the rift floor.

In the western part of Lake Abaya area, the $\delta^{18}\text{O}$ composition of groundwater shows irregular spatial variation and slight mineralization (EC up to 250 $\mu\text{S}/\text{cm}$), suggesting a dominance of the local recharge over the deep regional flow component. In this part of the study area, some of the groundwater from deep wells contains high concentrations of NO_3 , which suggests the downward percolation of water from the shallow groundwater flow system. The groundwater from the dissected highland enters into the valley, and the intermittent streams that drain the highland recharge the aquifer, which in turn resulted in the percolation of evaporated runoff, and consequently there is spatial variation in $\delta^{18}\text{O}$ distribution. The hot spring waters in the western part of Lake Abaya area show

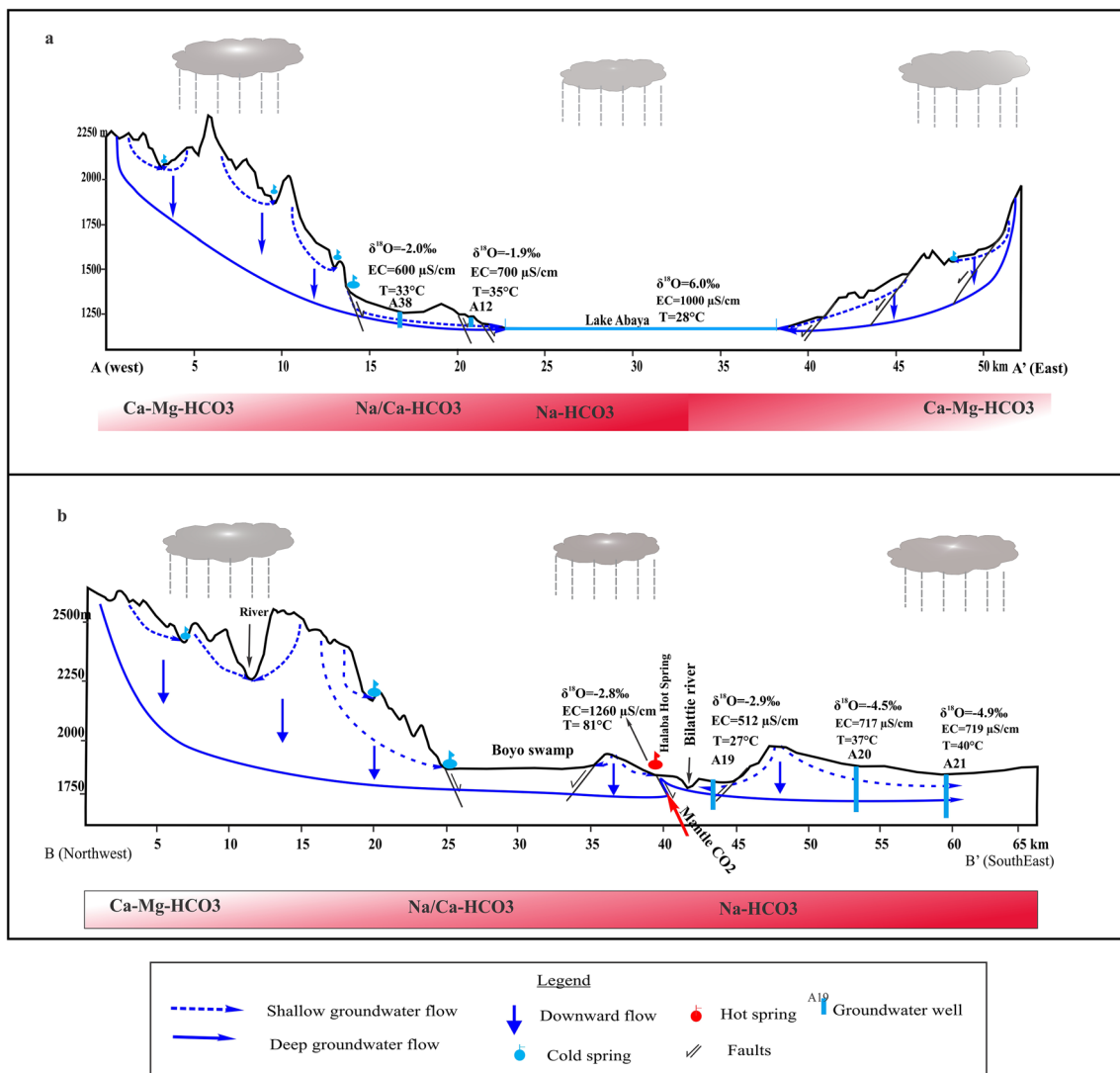


Fig. 11 Schematic cross section showing the hydrogeological conceptual model of the Abaya Chamo basin: **a** western part of Lake Abaya area and **b** northern part of the basin. The location of the cross-sections and their view direction are shown in Fig. 1

similar stable isotopic ($\delta^{18}\text{O}$) values to those of the groundwaters from the plateau in the west. The similarity of stable isotopic composition is observed in shallow and deep groundwaters, river water and rainwater, which suggests there is a good hydrological connection in the Abaya and Chamo lake basins, particularly in the western part of Lake Abaya area. It is observed that the local and regional groundwater flow is from W–E towards Lake Abaya.

In the northern part of the study area, the $\delta^{18}\text{O}$ composition of groundwater shows progressive depletion from highland to the rift floor. Likewise, significant changes in the concentration of the major ions occur in the flow direction of the northern part of the study area. The changes that occur along the flow direction include a progressive increase in temperature, EC, Na, F and HCO_3^- , starting from the mountains and travelling to the rift floor, with anomalous temperature and F around the town of Halaba and surrounding villages. The increase in groundwater temperature and major ions mirrors the increase in residence time and deep circulation. The groundwater temperature of the town of Halaba and surrounding villages is higher than the average temperature which is 27 °C, which suggests there is connection of these waters to deep regional groundwater circulation. This is consistent with their highly depleted $\delta^{18}\text{O}$ and δD isotope contents. Groundwater of shallow wells and deep wells on the western side of Bilatte River are relatively enriched in isotopic composition and slightly mineralized with uniform temperature (mean temperature 24 °C and mean F^- 0.6 mg/L). This indicates relatively good aquifer recharge, and the pore space has been flushed frequently to form slightly mineralized groundwater; however, groundwater samples east of the river are depleted in isotopic composition and they are highly mineralized (e.g. mean temperature 32 °C and mean F^- 4.2 mg/L), which suggests slow movement of groundwater, long residence time, deep-seated circulation, and only a small amount of precipitation that recharges the aquifer. On the other hand, this shows the role of normal faults in controlling groundwater flow systems. As Bilate River is rift-controlled (Molin and Corti 2015), compartmentalization of the flow system on the western side and eastern side is favored. Likewise, the other faults in the area favor the upward flow of deep thermal water along the fault zone, exemplified by high temperature and fluoride. This can be supported by the evidence shown on cross-section B–B' in Fig. 11b.

Conclusion

The spatial and temporal distribution of volcanic rocks, their structural relationship, and the abundance of heterogeneous reactive minerals makes the geochemical evolution and groundwater circulation in the rifted volcanic terrain of Ethiopia very complex. The present study has demonstrated that the application of hydrochemical data, together with multi-isotopic techniques, enabled the groundwater chemical

evolution to be characterized and the groundwater circulation in the volcanic aquifers of Abaya Chamo basin to be schematized.

The hydrochemistry of groundwater in the basin is largely explained by the geochemical processes of silicate hydrolysis and cation exchange. The hydrochemical signature shows the spatial variation in ionic concentration, where Na^+ is the dominant cation and HCO_3^- is the dominant anion. From the highland towards the Rift floor, groundwater evolves from Ca-Mg- HCO_3^- type to Na- HCO_3^- type. Groundwater samples collected from the western part of Lake Abaya area are predominantly Ca-Mg- HCO_3^- type, while those collected from the northern part of the area are predominantly Na- HCO_3^- type. Groundwater composition is directly related to water–rock interactions, mainly due to the dissolution of silicate minerals in the presence of CO_2 , leading to the release of Na^+ , K^+ , Mg^{2+} , Ca^{2+} , and HCO_3^- to the groundwater.

Groundwater of the study area is of meteoric origin, with the range -4.9 to -1.1‰ VSMOW for $\delta^{18}\text{O}$ and -27 to 5‰ VSMOW for δD . The $\delta^{18}\text{O}$ and δD content of groundwater in the basin lies on the summer LMWL, which indicates that the groundwater is mainly recharged by summer rainfall.

$\delta^{13}\text{C}_{\text{DIC}}$ values of all water samples range from -12.0 to $+1.6\text{‰}$ (VPDB). The $\delta^{13}\text{C}_{\text{CO}_2(\text{g})}$ content was calculated using $\delta^{13}\text{C}_{\text{DIC}}$ and the measured hydrochemical parameter HCO_3^- , and it clearly indicates that (1) biogenic soil CO_2 is a dominant source of dissolved inorganic carbon (DIC) in the low mineralized groundwater and (2) thermal water had mostly mantle-derived magmatic CO_2 . A low $\delta^{13}\text{C}_{\text{CO}_2}$ value was found in groundwater from the western part of Lake Abaya area, and enriched $\delta^{13}\text{C}_{\text{CO}_2}$ was found in the northern part of the study area.

Two regional groundwater flow systems were established based on analysis of $\delta^{18}\text{O}$, $\delta^{13}\text{C}_{\text{DIC}}$ and major ions. Regardless of the geological framework, the variability of the chemical composition of groundwater samples from the northern part is significant; in the western part of Lake Abaya area, the chemical content of groundwater becomes homogeneous and the concentrations are smaller than in the northern part. Groundwater samples along the northern part of the area contain low $\delta^{18}\text{O}$, enriched $\delta^{13}\text{C}$, and high F, and the spatial differences in $\delta^{18}\text{O}$, $\delta^{13}\text{C}$ and major ions suggest sluggish groundwater movement, including local compartmentalization of the flow system. In the western part of Lake Abaya region, shallow and deep groundwater flow systems are connected from highland to lowland areas, by considering consistent $\delta^{18}\text{O}$ values and major ion contents throughout the area. Groundwater in the western part of Lake Abaya area shows low $\delta^{13}\text{C}_{\text{CO}_2}$ values, which reflects the high contribution of local recharge through the soil layer, mixing of water with different sources and fast circulation.

Integration of data on multiple isotopes and solutes in groundwater with interpretation of the volcanic stratigraphy reveals the complicated patterns of water–rock interactions

and circulation in the volcanic aquifers. This study has implications for understanding groundwater flow dynamics as well as chemical evolution of groundwater in volcanic aquifers, which are major sources of drinking water in many parts of the world. The conceptualization of the flow system established in this study is expected to play a vital role in finding suitable sites for future groundwater development within the Abaya Chamo basin.

Acknowledgments This report is based on the PhD study of the first author at the Chinese Academy of Science, Institute of Geology and Geophysics (IGGCAS). IGGCAS (Institute of Geology and Geophysics, Chinese Academy of Science) is gratefully acknowledged for managing the grant and facilitating field works in Ethiopia. We thank the editor (Dr. Jean-Michel Lemieux) and three anonymous reviewers for their helpful comments in improving the manuscript.

Funding information CAS-TWAS President's Fellowship program is acknowledged for a PhD research grant to the first author.

References

- Adams S, Titus R, Pietersen K, Tredoux G, Harris C (2001) Hydrochemical characteristics of aquifers near Sutherland in the Western Karoo, South Africa. *J Hydrol* 241(1):91–103
- Ahmed A, Clark I (2016) Groundwater flow and geochemical evolution in the Central Flinders Ranges, South Australia. *Sci Total Environ* 572:837–851
- Ako AA, Shimada J, Hosono T, Kagabu M, Richard A, Nkeng GE, Tongwa AF, Ono M, Eyong GET, Tandia BK, Mouchereou OF (2013) Flow dynamics and age of groundwater within a humid equatorial active volcano (Mount Cameroon) deduced by δD , $\delta^{18}O$, $3H$ and chlorofluorocarbons (CFCs). *J Hydrol* 502:156–176
- Alemayehu T (2006) Groundwater occurrence in Ethiopia. UNESCO, Paris
- Alemayehu T, Leis A, Eisenhauer A, Dietzel M (2011) Multi-proxy approach ($2H/H$, $18O/16O$, $13C/12C$ and $87Sr/86Sr$) for the evolution of carbonate-rich groundwater in basalt dominated aquifer of Axum area, northern Ethiopia. *Chem Erde - Geochem* 71(2):177–187
- Appelo CAJ, Postma D (2005) *Geochemistry: groundwater and pollution*, Taylor and Francis, London
- Asai K, Satake H, Tsujimura M (2009) Isotopic approach to understanding the groundwater flow system within an andesitic stratovolcano in a temperate humid region: case study of Ontake Volcano, central Japan. *Hydrol Process* 23(4):559–571
- Ayewew T (2008) The distribution and hydrogeological controls of fluoride in the groundwater of central Ethiopian Rift and adjacent highlands. *Environ Geol* 54(6):1313–1324
- Ayewew T, Demlie M, Wöhrlich S (2008) Hydrogeological framework and occurrence of groundwater in the Ethiopian aquifers. *J Afr Earth Sci* 52:97–113
- Belkhir L, Mouni L, Boudoukha A (2012) Geochemical evolution of groundwater in an alluvial aquifer: case of El Eulma aquifer, East Algeria. *J Afr Earth Sci* 66–67:46–55
- Bertrand G, Celle-Jeanton H, Huneau F, Loock S, Renac C (2010) Identification of different groundwater flowpaths within volcanic aquifers using natural tracers for the evaluation of the influence of lava flows morphology (Argnat basin, Chaîne des Puys, France). *J Hydrol* 391:223–234
- Bertrand G, Celle-Jeanton H, Loock S, Huneau F, Lavastre V (2013) Contribution of PCO_2 eq and $13CTDIC$ evaluation to the identification of CO_2 sources in volcanic groundwater systems: influence of hydrometeorological conditions and lava flow morphologies—application to the Argnat Basin (Chaîne des Puys, Massif Central, France). *Aquatic Geochem* 19(2):147–171
- Bretzler A, Osenbrück K, Gloaguen R, Ruprecht JS, Kebede S, Stadler S (2011) Groundwater origin and flow dynamics in active rift systems: a multi isotope approach in the Main Ethiopian Rift—a multi-proxy approach. *J Hydrol* 402:274–289
- Carrillo-Rivera JJ, Varsányi I, Kovács LÓ, Cardona A (2007) Tracing groundwater flow systems with hydrogeochemistry in contrasting geological environments. *Water Air Soil Pollut* 184(1–4):77–103
- Cartwright I, Weaver T, Tweed S, Ahearn D, Cooper M, Czapnik K, Tranter J (2002) Stable isotope geochemistry of cold CO_2 -bearing mineral spring waters, Daylesford, Victoria, Australia: sources of gas and water and links with waning volcanism. *Chem Geol* 185(1):71–91
- Cerling TE, Harris JMJO (1999) Carbon isotope fractionation between diet and bioapatite in ungulate mammals and implications for ecological and paleoecological studies. *120(3):347–363*
- Chernet T (2011) Geology and hydrothermal resources in the northern Lake Abaya Area (Ethiopia). *J Afr Earth Sci* 61(2):129–141
- Chernet T, Travi Y, Valles V (2001) Mechanism of degradation of the quality of natural water in the lakes region of the Ethiopian Rift Valley. *Water Res* 35(12):2819–2832
- Clark I (2015) *Groundwater geochemistry and isotopes*. CRC, Boca Raton, FL
- Clark ID, Fritz P (1997) *Environmental isotopes in hydrogeology*. CRC, Boca Raton, FL
- Cordeiro S, Coutinho R, Cruz JV (2012) Fluoride content in drinking water supply in Sao Miguel volcanic island (Azores, Portugal). *Sci Total Environ* 432:23–36
- Corti G (2009) Continental rift evolution: from rift initiation to incipient break-up in the Main Ethiopian Rift, East Africa. *Earth-Sci Rev* 96(1–2):1–53
- Corti G, Sani F, Philippon M, Sokoutis D, Willingshofer E, Molin P (2013) Quaternary volcano-tectonic activity in the Soddo region, western margin of the southern Main Ethiopian Rift. *Tectonics* 32(4):861–879
- Craig H, Lupton JE, Horowitz R M (1977) Isotopic geochemistry and hydrology of geothermal waters in the Ethiopian Rift Valley. Scripps Institute of Oceanography, University of California, San Diego
- Cruz JV, França Z (2006) Hydrogeochemistry of thermal and mineral water springs of the Azores archipelago (Portugal). *J Volcanol Geothermal Res* 151(4):382–398
- Cruz JV, Silva O (2001) Hydrogeologic framework of Pico Island, Azores, Portugal. *Hydrogeol J* 9(2):177–189
- Dafny E, Gvirtzman H, Burg A, Fleischerc L (2003) The hydrogeology of the Golan basalt aquifer, Israel. *Israel J Earth Sci* 52:139–153
- Darling WG, Gizaw B, Arusei MK (1996) Lake–groundwater relationships and fluid–rock interaction in the East African Rift Valley: isotopic evidence. *J Afr Earth Sci* 22(4):423–431
- Deines P, Langmuir D, Harmon RS (1974) Stable carbon isotope ratios and the existence of a gas phase in the evolution of carbonate ground waters. *Geochim Cosmochim Acta* 38(7):1147–1164
- Demlie M, Wöhrlich S, Gizaw B, Stiehler W (2007) Groundwater recharge in the Akaki catchment, central Ethiopia: evidence from environmental isotopes ($\delta^{18}O$, δ^2H and $3H$) and chloride mass balance. *Hydrol Process* 21(6):807–818
- Demlie M, Wöhrlich S, Ayewew T (2008) Major ion hydrochemistry and environmental isotope signatures as a tool in assessing groundwater occurrence and its dynamics in a fractured volcanic aquifer system located within a heavily urbanized catchment, central Ethiopia. *J Hydrol* 353:175–188
- Dietzel M, Kirchhoff T (2002) Stable isotope ratios and the evolution of acidulous ground water. *Aquatic Geochem* 8(4):229–254

- Ebinger CJ, Yemane T, WoldeGabriel G, Aronson JL, Walter RC (1993) Late Eocene–Recent volcanism and faulting in the southern Main Ethiopian Rift. *J Geol Soc* 150(1):99–108
- Elango L, Kannan R (2007) Rock–water interaction and its control on chemical composition of groundwater, chap 11. In: Sarkar D, Datta R, Hannigan R (eds) *Developments in environmental science*, vol 5. Elsevier, Amsterdam, pp 229–243
- Elango L, Kannan R, Senthil Kumar M (2003) Major ion chemistry and identification of hydrogeochemical processes of ground water in a part of Kancheepuram district, Tamil Nadu, India. *Environ Geosci* 10(4):157–166
- Furi W, Razack M, Abiye TA, Ayenew T, Legesse D (2011) Fluoride enrichment mechanism and geospatial distribution in the volcanic aquifers of the Middle Awash basin, Northern Main Ethiopian Rift. *J Afr Earth Sci* 60(5):315–327
- Furi W, Razack M, Haile T, Abiye TA, Legesse D (2010) The hydrogeology of Adama-Wonji basin and assessment of groundwater level changes in Wonji wetland, Main Ethiopian Rift: results from 2D tomography and electrical sounding methods. *Environ Earth Sci* 62(6):1323–1335
- Gastmans D, Hutcheon I, Menegário AA, Chang HK (2016) Geochemical evolution of groundwater in a basaltic aquifer based on chemical and stable isotopic data: case study from the northeastern portion of Serra Geral Aquifer, São Paulo state (Brazil). *J Hydrol* 535:598–611
- Genereux DP, Webb M, Solomon DK (2009) The chemical and isotopic signature of old groundwater and magmatic solutes in a Costa Rican rainforest: evidence from carbon, helium, and chlorine. *Water Resour Res* 45:W08413
- Gizaw B (1996) The origin of high bicarbonate and fluoride concentrations in waters of the Main Ethiopian Rift Valley, East African Rift System. *J Afr Earth Sci* 22(4):391–402
- Haile T, Abiye TA (2012) The interference of a deep thermal system with a shallow aquifer: the case of Sodere and Gerged thermal springs, Main Ethiopian Rift, Ethiopia. *Hydrogeol J* 20(3):561–574
- Haji M, Wang D, Li L, Qin D, Guo Y (2018, 1799) Geochemical evolution of fluoride and implication for F-enrichment in groundwater: example from the Bilate River Basin of Southern Main Ethiopian Rift. *Water* 10(12):1799. <https://doi.org/10.3390/w10121799>
- Halcrow (2008) Rift Valley Lakes basin integrated natural resources development master plan. Ethiopian Valleys Development Studies Authorities, Ministry of Water Resources, Addis Ababa, Ethiopia
- Hoefs J (2009) *Stable isotope geochemistry*. Springer, Heidelberg, Germany
- JICA (2012) The study on groundwater resources assessment in the Rift Valley Lakes Basin in the Federal Democratic Republic of Ethiopia. Japan International Cooperation Agency (JICA), Kokusai Kogyo, Ministry of Water and Energy (MoWE), Tokyo
- Kebede S (2013) *Groundwater in Ethiopia: features, numbers and opportunities*. Springer, Heidelberg, Germany, 283 pp
- Kebede S, Travi Y, Alemayehu T, Ayenew T (2005) Groundwater recharge, circulation and geochemical evolution in the source region of the Blue Nile River, Ethiopia. *Appl Geochem* 20(9):1658–1676
- Kebede S, Travi Y, Asrat A, Alemayehu T, Ayenew T, Tessema Z (2008) Groundwater origin and flow along selected transects in Ethiopian rift volcanic aquifers. *Hydrogeol J* 16:55–73
- Kebede S, Travi Y, Stadler S (2010) Groundwaters of the central Ethiopian rift: diagnostic trends in trace elements, d18O and major elements. *Environ Earth Sci* 61:1641–1655
- Kebede S, Hailu A, Crane E, Dochartaigh Ó, Dochartaigh BÉ (2016) *Africa groundwater atlas: hydrogeology of Ethiopia*. British Geological Survey, Keyworth, UK, pp 1–17
- Koh D-C, Chae G-T, Yoon Y-Y, Kang B-R, Koh G-W, Park K-H (2009) Baseline geochemical characteristics of groundwater in the mountainous area of Jeju Island, South Korea: implications for degree of mineralization and nitrate contamination. *J Hydrol* 376(1–2):81–93
- Koh D-C, Genereux DP, Koh G-W, Ko K-S (2017) Relationship of groundwater geochemistry and flow to volcanic stratigraphy in basaltic aquifers affected by magmatic CO₂, Jeju Island, Korea. *Chem Geol* 467:143–158
- Kulkarni H, Deolankar SB, Lalwani A, Joseph B, Pawar S (2000) Hydrogeological framework of the Deccan basalt groundwater systems, west-central India. *Hydrogeol J* 8(4):368–378
- Lamb HF, Melanie JL, Richard JT, Tenalem A, Mohammed U (2007) Oxygen and carbon isotope composition of authigenic carbonate from an Ethiopian lake: a climate record of the last 2000 years. *Holocene* 17(4):517–526
- Li C, Gao X, Wang Y (2015) Hydrogeochemistry of high-fluoride groundwater at Yuncheng Basin, northern China. *Sci Total Environ* 508:155–165
- Marini L, Ottonello G, Canepa M, Cipolli F (2000) Water–rock interaction in the Bisagno Valley (Genoa, Italy): application of an inverse approach to model spring water chemistry. *Geochim Cosmochim Acta* 64(15):2617–2635
- Mechal A, Birk S, Dietzel M, Leis A, Winkler G, Mogessie A, Kebede S (2016) Groundwater flow dynamics in the complex aquifer system of Gidabo River Basin (Ethiopian Rift): a multi-proxy approach. *Hydrogeol J* 25(2):519–538
- Minissale A, Corti G, Tassi F, Darrah TH, Vaselli O, Montanari D, Montegrossi G, Yirgu G, Selmo E, Teclu A (2017) Geothermal potential and origin of natural thermal fluids in the northern Lake Abaya area, Main Ethiopian Rift, East Africa. *J Volcanol Geothermal Res* 336:1–18
- Molin P, Corti G (2015) Topography, river network and recent fault activity at the margins of the Central Main Ethiopian Rift (East Africa). *Tectonophysics* 664:67–82
- Mook WG, Bommerson JC, Staverman WH (1974) Carbon isotope fractionation between dissolved bicarbonate and gaseous carbon dioxide. *Earth Planet Sci Lett* 22(2):169–176
- Möller P, Rosenthal E, Inbar N, Magri F (2016) Hydrochemical considerations for identifying water from basaltic aquifers: the Israeli experience. *J Hydrol* 5:33–47
- Négrel P, Petelet-Giraud E, Millot R (2016) Tracing water cycle in regulated basin using stable δ18O–δ2H isotopes: the Ebro River basin (Spain). *Chem Geol* 422:71–81
- Ochoa-González GH, Carreón-Freyre D, Cerca M, López-Martínez M (2015) Assessment of groundwater flow in volcanic faulted areas: a study case in Queretaro, Mexico. *Geofis Int* 54(3):199–220
- Olaka LA, Wilke FD, Olago DO, Odada EO, Mulch A, Musolf A (2016) Groundwater fluoride enrichment in an active rift setting: central Kenya Rift case study. *Sci Total Environ* 545–546:641–653
- Prada S, Cruz JV, Figueira C (2016) Using stable isotopes to characterize groundwater recharge sources in the volcanic island of Madeira, Portugal. *J Hydrol* 536:409–425
- Qin D, Zhao Z, Guo Y, Liu W, Haji M, Wang X, Xin B, Li Y, Yang Y (2017) Using hydrochemical, stable isotope, and river water recharge data to identify groundwater flow paths in a deeply buried karst system. *Hydrol Process* 31(24):4297–4314
- Rango T, Bianchini G, Beccaluva L, Ayenew T, Colombani N (2008) Hydrogeochemical study in the Main Ethiopian Rift: new insights to the source and enrichment mechanism of fluoride. *Environ Geol* 58(1):109–118
- Rango T, Petrini R, Stenni B, Bianchini G, Slejko F, Beccaluva L, Ayenew T (2010) The dynamics of central Main Ethiopian Rift waters: evidence from dD, d18O and 87Sr/86Sr ratios. *Appl Geochem* 25:1860–1871
- Rango T, Kravchenko J, Atlaw B, McCormick PG, Jeuland M, Merola B, Vengosh A (2012) Groundwater quality and its health impact: an assessment of dental fluorosis in rural inhabitants of the Main Ethiopian Rift. *Environ Int* 43:37–47
- Rappich V, Žáček V, Verner K, Erban V, Goslar T, Bekele Y, Legesa F, Hroch T, Hejtánková P (2016) Wendo Koshe Pumice: the latest

- Holocene silicic explosive eruption product of the Corbetti Volcanic System (southern Ethiopia). *J Volcanol Geotherm Res* 310:159–171
- Reimann C, Bjorvatn K, Frengstad B, Melaku Z, Tekle-Haimanot R, Siewers U (2003) Drinking water quality in the Ethiopian section of the East African Rift Valley, I: data and health aspects. *Sci Total Environ* 311:65–80
- Rooney TO, Bastow ID, Keir D (2011) Insights into extensional processes during magma assisted rifting: evidence from aligned scoria cones. *J Volcanol Geotherm Res* 201(1–4):83–96
- Shoeller H (1967) Geochemistry of groundwater. In: Brown RH, Konoplyantsev AA, Ineson J, Kovalevsky VS (eds) *Groundwater studies: an international guide for research and practice*. UNESCO, Paris, pp 1–18
- Tardy Y (1971) Characterization of the principal weathering types by the geochemistry of waters from some European and African crystalline massifs. *Chem Geol* 7(4):253–271
- Tekle-Haimanot R, Haile G (2014) Chronic alcohol consumption and the development of skeletal fluorosis in a fluoride endemic area of the Ethiopian Rift Valley. *J Water Resour Protect* 06(02):149–155
- Tekle-Haimanot R, Melaku Z, Kloos H, Reimann C, Fantaye W, Zerihun L, Bjorvatn K (2006) The geographic distribution of fluoride in surface and groundwater in Ethiopia with an emphasis on the Rift Valley. *Sci Total Environ* 367(1):182–190
- UNDP (1973) *Geology geochemistry and hydrology of Hot Springs of the East African systems within Ethiopia*. United Nations Development Programme, New York
- Vaselli O, Minissale A, Tassi F, Magro G, Seghedi I, Ioane D, Szakacs A (2002) A geochemical traverse across the Eastern Carpathians (Romania): constraints on the origin and evolution of the mineral water and gas discharges. *Chem Geol* 182(2):637–654
- Vivona R, Preziosi E, Madé B, Giuliano G (2007) Occurrence of minor toxic elements in volcanic-sedimentary aquifers: a case study in central Italy. *Hydrogeol J* 15(6):1183–1196
- Vogel JC, Grootes PM, Mook WG (1970) Isotopic fractionation between gaseous and dissolved carbon dioxide. *Zeitschrift Physik A Hadrons Nuclei* 230(3):225–238
- WoldeGabriel G, Aronson JL, Walter RC (1990) Geology, geochronology, and rift basin development in the central sector of the Main Ethiopia Rift. *Geol Soc Am Bull* 102(4):439
- WoldeGabriel G, Yemane T, Suwa G, White T, Asfaw B (1991) Age of volcanism and rifting in the Burji-Soyoma area, Amaro Horst, southern Main Ethiopian Rift: geo- and biochronologic data. *J Afr Earth Sci* 13(3):437–447
- Wondwossen F, Åström AN, Bjorvatn K, Bårdsen A (2004) The relationship between dental caries and dental fluorosis in areas with moderate- and high-fluoride drinking water in Ethiopia. *Commun Dentistry Oral Epidemiol* 32(5):337–344
- Zanettin B, Justin-Visentin E, Nicoletti M, Petrucciani C (1978) The evolution of Chenchu escarpment and Ganjule Graben in Southern Ethiopia Rift. *N Jb Geol Palaont Mh* (8):473–490
- Zinabu GM, Kebede-Westhead E, Desta Z (2002) Long-term changes in chemical features of waters of seven Ethiopian Rift-Valley lakes. *Hydrobiologia* 477(1):81–91

Publisher's note Springer Nature remains neutral with regard to jurisdictional claims in published maps and institutional affiliations.